Available online at http://scik.org
Commun. Math. Biol. Neurosci. 2022, 2022:106
https://doi.org/10.28919/cmbn/7722
ISSN: 2052-2541

MODELING AND ANALYSIS OF A PREY-PREDATOR SYSTEM INCORPORATING FEAR, PREDATOR-DEPENDENT REFUGE, AND CANNIBALISM

AHMED SAMI ABDULGHAFOUR[1], RAID KAMEL NAJI[2,*]

[1]Scientific Affairs Department, Al-Iraqia University, Baghdad, Iraq

[2]Department of Mathematics, College of Science, University of Baghdad, Baghdad, Iraq

Abstract: Using a mathematical model to simulate the interaction between prey and predator was suggested and researched. It was believed that the model would entail predator cannibalism and constant refuge in the predator population, while the prey population would experience predation fear and need for a predator-dependent refuge. This study aimed to examine the proposed model's long-term behavior and explore the effects of the model's key parameters. The model's solution was demonstrated to be limited and positive. All potential equilibrium points' existence and stability were tested. When possible, the appropriate Lyapunov function was utilized to demonstrate the equilibrium points' overall stability. The system's persistence requirements were specified. The circumstances of local bifurcation that could take place close to the equilibrium points were discovered. Numerical simulations were run to validate the model's obtained long-term behavior and comprehend the effects of the model's key parameters in order to confirm our analytical conclusions. It has been observed that the system may have numerous coexistence equilibrium points, leading to bi-stable behavior. The fear rate reduces the multiplicity of the equilibrium point and converts the bi-stable

[*]Corresponding author
E-mail address: rknaji@gmail.com
Received September 08, 2022

situation into a stable case, which stabilizes the system (1) up to the top particular value.

Keywords: prey-predator; predator cannibalism; a refuge; fear; stability; bifurcation.

2010 AMS Subject Classification: 34C23, 34D20, 92D40.

1. INTRODUCTION

Many different species interact with one another. Direct encounters do occur. However, a large number of exchanges are indirect and so less noticeable. The fact that changes in one species, such as changes in its population size, health, or geographic distribution, will almost surely have an impact on other species and other elements of the Earth system is a result of the direct and indirect interactions between species. Prey-predator interactions, which are the most frequent interactions in the environment, occur when two creatures of different species engage and one of them behaves as a predator, catching and eating the other organism that is the prey. Predation is a method of population control in ecology. Therefore, more prey should be present when there are fewer predators. The predators would therefore be able to multiply more and perhaps alter their hunting strategies. The number of prey decreases as the number of predators increases. This causes food shortages for predators, which may ultimately result in the demise of numerous predators.

Since the groundbreaking work of the Lotka-Volterra model, prey-predator relationships have become a crucial field for scientists because of their widespread existence. The dynamical behavior of the prey-predator systems has been the subject of numerous studies that have been published in order to understand and study it, see for example [1-4]. Prey refuge is one of the most crucial element influencing the dynamic behavior of the prey-predator system. In order to evade predators, the prey seeks refuge. In various dynamic systems, the usage of refuge by prey in response to a predator attack is observed. The dynamics of prey-predator systems with prey refuge are studied using a variety of mathematical models [5–13].

The practice of eating another member of the same species as food is known as cannibalism. In the animal kingdom, cannibalism is a frequent ecological interaction that has been seen in more than 1500 species [14]. Because animal turn to their fellow species as a second source of sustenance in circumstances with inadequate nutrition, the rate of cannibalism rises. Cannibalism controls population growth by reducing possible competition for resources like food, shelter, and territory, which makes them more accessible. It has been demonstrated that the prevalence of cannibalism lowers the predicted survival rate of the entire group and raises the chance of consuming a relative, despite the fact that it may benefit the individual. As the frequency of encounters between hosts rises, there may be additional detrimental impacts, such as an increased risk of disease transmission. However, contrary to what was long believed, cannibalism can occur in a range of species in their natural habitats, not just in situations where there is a severe lack of food or under artificial or unnatural conditions. Consequently, researchers have looked at a number of mathematical models of cannibalism or intraspecific predation [15-22]. Since many species in nature exhibit cannibalistic behaviors, especially in aquatic environments, a prey-predator model containing cannibalism is interesting to research.

On the other hand, the indirect impact of predation on the life and reproduction of the prey owing to the fear of predation is equal to or greater than the direct impact caused by the predators' actual death of the prey. The influence of fear on prey populations must be taken into account since there are instances when the presence of fear leads to antipredator behavior that negatively affects the predator population and forces prey to temporarily leave their habitat or foraging area [23]. Several mathematical models considered the impact of fear on the prey-predator interaction, see for example [12, 13, 24-30]. Additionally, Diz-Pita and Otero-Espinar [31] provide additional research on prey-predator systems incorporating several biological variables.

Rayungsari et al. [32] recently created and investigated a mathematical model to describe the interaction between predator and prey that incorporates predator cannibalism and refuge using the Holling type II functional response to describe the predation processes. The Beddington-DeAngelis type of functional response was used by Jamil and Naji [13] to propose and investigate the impacts of fear, quadratic fixed effort harvesting, and predator-dependent refuge on a modified Leslie-Gower prey-predator model. However, in this study, a Holling type II prey-predator system is created by combining predator cannibalism, predation fear, constant predator refuge, and predator-dependent refuge.

2. MODEL FORMULATION

This section proposes a mathematical model of prey-predator incorporating fear, predator-dependent refuge, and cannibalism depending on the following assumptions.

In the absence of the predator, it is thought that the prey multiplies logistically while the predator species degenerates exponentially without food. The functional response of type II of Holling describes the transition of food from the prey to the predator. The predator's ability to cannibalize weaker predator species provides them with a second supply of food. The prey also hides in a variety of shelters that rely on their contact with the predator species, and their fear of predation affects how they give birth. According to these assumptions the dynamic system of such a prey-predator system can be represented by the following two equations:

$$\begin{aligned} \frac{dX}{dt} &= X\left(\frac{r}{1+fY} - d_1 - bX - \frac{a_1(1-cY)Y}{K_1+X(1-cY)}\right) = G_1(X,Y) = Xg_1(X,Y), \\ \frac{dY}{dt} &= Y\left(\frac{a_2X(1-cY)}{K_1+X(1-cY)} + a_3 - d_2 - \frac{e(1-m)Y}{K_2+(1-m)Y}\right) = G_2(X,Y) = Yg_2(X,Y), \end{aligned} \tag{1}$$

where all the coefficients are positive constants and can be described in table (1).

Table 1: parameters description.

Parameter	Description
r	The prey birth rate
d_1	The prey's natural death rate
b	The prey intraspecific competition
f	The prey's fear level, which is involved in the fear function $\frac{1}{1+fY}$.
a_1	The attack rate
K_1	The half-saturation constant.
$c \in [0,1]$	The prey's refuge rate; hence the refuge amount is cXY, which leaves $X(1-cY)$ of the prey available to be hunted by the predator
a_2	The conversion rate of prey biomass into predator birth
a_3	The conversion rate of cannibalism into predator birth
d_2	The predator's natural death rate
$m \in [0,1]$	The predator refuge rate; hence $(1-m)Y$ of predator is available for cannibalism.
e	The cannibalism rate in predators.
K_2	The half-saturation constant of cannibalism

3. Preliminaries Results

From the form of interaction functions $G_1(X,Y)$, and $G_2(X,Y)$ given in system (1), they are continuous and have continuous partial derivatives on the region $\Omega = \{(X,Y) \in \mathbb{R}_+^2 : X \geq 0, Y \geq 0\}$. Hence these functions are locally Lipschitz on Ω. Consequently, using the fundamental existence and uniqueness theorem [33], we obtain that for the system (1) with any non-negative initial condition $X(0) \geq 0$, and $Y(0) \geq 0$ there exists $T > 0$ so that the system (1) has a unique solution defined in Ω.

Note that the solution of system (1) must be non-negative because the variables in the system indicate population densities. Then the following theorem ensures that the solution of system (1) is non-negative.

Theorem 1: All system (1) solutions with initial values $(X(0), Y(0))$ belonging to Ω are non-negative.

Proof: By solving the equations in the system (1), using the given initial value yields that:

$$X(t) = X(0)e^{\int_0^t \left(\frac{r}{1+fY(u)} - d_1 - bX(u) - \frac{a_1(1-cY(u))Y(u)}{K_1+X(u)(1-cY(u))}\right)du}$$

Similarly,

$$Y(t) = Y(0)e^{\int_0^t \left(\frac{a_2X(u)(1-cY(u))}{K_1+X(u)(1-cY(u))} + a_3 - d_2 - \frac{e(1-m)Y(u)}{K_2+(1-m)Y(u)}\right)du}$$

Therefore, if $X(0) = 0$, and $Y(0) = 0$ then it is obtained that $X(t) = Y(t) = 0$ all the time. Otherwise, $X(t) \geq 0$, and $Y(t) \geq 0$ indefinitely due to the positivity of the exponential function in the above two equations.

On the other hand, the populations in system (1) must be limited due to the limited resources in the environment.

Theorem 2: All solutions of system (1) with initial values $(X(0), Y(0))$ belonging to Ω are uniformly bounded.

Proof: From the first equation of the system (1), it is obtained that

$$\frac{dX}{dt} \leq (r - d_1)X - bX^2 = \delta X - bX^2,$$

where $\delta = (r - d_1) > 0$, represents the prey survival condition. Therefore, for $t \to \infty$, it was obtained that $X(t) \leq \frac{\delta}{b} = \sigma_1$.

Let $W(t) = X(t) + Y(t)$, then by derivative, the following is obtained:

$$\frac{dW}{dt} = \frac{dX}{dt} + \frac{dY}{dt} \leq (r - d_1)X + (a_3 - d_2)Y = \delta X - \beta Y,$$

where $\beta = d_2 - a_3 > 0$. Further simplifications yields that

$$\frac{dW}{dt} + \beta W \leq (\delta + \beta)\sigma_1.$$

Accordingly, it is easy to verify that the solution of the above first-order differential inequality satisfies that:

$$W(t) \leq \frac{(\delta+\beta)\sigma_1}{\beta} + \left(W(0) - \frac{(\delta+\beta)\sigma_1}{\beta}\right) e^{-\beta t}.$$

Since $\lim_{t\to\infty} e^{-\beta t} = 0$, hence for $t \to \infty$, it is obtained that $W(t) \leq \frac{(\delta+\beta)\sigma_1}{\beta} = \sigma_2$, which shows that all the solutions are uniformly bounded.

4. STABILITY ANALYSIS

System (1) has the following set of equilibrium points, which is obtained by equating the system to zero.

The vanishing equilibrium point (VEP) that is given by $E_1 = (0,0)$, always exists.

The first axial equilibrium point (FAEP) is written as $E_2 = (h_1, 0)$, where $h_1 = \frac{r-d_1}{b}$ exists provided that

$$r - d_1 > 0. \tag{2}$$

The second axial equilibrium point (SAEP) is written as $E_3 = (0, h_2)$, where $h_2 = \frac{(d_2-a_3)K_2}{[a_3-d_2-e](1-m)}$ exists provided that

$$d_2 < a_3 < d_2 + e \tag{3}$$

In the event that the conversion rate of cannibalism into predator birth is higher than their natural death rate and lower than the total cannibalism rate in predators and their natural death rate, the predator will continue to exist even if the prey is extinct.

The coexistence equilibrium point (COEP) is given by $E_4 = (X^*, Y^*)$, where

$$X^* = \frac{K_1[e(1-m)Y^*-(a_3-d_2)(K_2+(1-m)Y^*)]}{(1-cY^*)[(a_2+a_3-d_2)(K_2+(1-m)Y^*)-e(1-m)Y^*]}, \tag{4}$$

while Y^* is a positive root of the following six-order equation.

$$\Delta_1 Y^6 + \Delta_2 Y^5 + \Delta_3 Y^4 + \Delta_4 Y^3 + \Delta_5 Y^2 + \Delta_6 Y + \Delta_7 = 0, \tag{5}$$

where

$$\Delta_1 = -[(e-a_2)-(a_3-d_2)]^2 c^2 f(1-m)^2 a_1 < 0.$$

$$\Delta_7 = [(a_2+a_3-d_2)(r-d_1)+bK_1(a_3-d_2)]a_2 K_1 K_2^2 > 0,$$

while the other coefficients are determined and given in appendix A.

The COEP exists in the interior of the state-space Ω provided that:

$$\frac{e(1-m)Y^*}{(a_2+a_3-d_2)} < (K_2+(1-m)Y^*) < \frac{e(1-m)Y^*}{(a_3-d_2)}. \tag{6}$$

With one set of the following sets of conditions.

$$\left.\begin{array}{l} \Delta_2 < 0, \Delta_3 < 0, \Delta_4 < 0, \Delta_5 < 0, \Delta_6 < 0, \\ \Delta_2 > 0, \Delta_3 > 0, \Delta_4 > 0, \Delta_5 > 0, \Delta_6 > 0, \\ \Delta_2 < 0, \Delta_3 < 0, \Delta_4 \neq 0, \Delta_5 > 0, \Delta_6 > 0, \\ \Delta_2 < 0, \Delta_3 < 0, \Delta_4 < 0, \Delta_5 < 0, \Delta_6 > 0, \\ \Delta_2 < 0, \Delta_3 > 0, \Delta_4 > 0, \Delta_5 > 0, \Delta_6 > 0 \end{array}\right\} \tag{7}$$

Now, the local stability analysis is carried out by computing the Jacobian matrix (JM) of the system (1) and determining their eigenvalues at each of the above-determined EPs. Consider the JM at the point (X, Y) that can be written as:

$$J = \begin{bmatrix} j_{11} & j_{12} \\ j_{21} & j_{22} \end{bmatrix} \tag{8}$$

where:

$$j_{11} = X\left[\frac{a_1 Y(1-cY)^2}{[K_1+X(1-cY)]^2} - b\right] + g_1(X,Y);$$

$$j_{12} = -X\left[\frac{K_1 a_1(1-2cY)+a_1 X(1-cY)^2}{[K_1+X(1-cY)]^2} + \frac{rf}{(1+fY)^2}\right],$$

$$j_{21} = \mathrm{Y}\left[\frac{K_1 a_2(1-cY)}{[K_1+X(1-cY)]^2}\right],$$

$$j_{22} = -Y\left[\frac{K_1 a_2 cX}{[K_1+X(1-cY)]^2} + \frac{K_2 e(1-m)}{[K_2+(1-m)Y]^2}\right] + g_2(X,Y).$$

Consequently, the JM at the VEP can be written as:

$$J_{E_1} = \begin{bmatrix} r-d_1 & 0 \\ 0 & a_3-d_2 \end{bmatrix}. \tag{9}$$

Hence the eigenvalues are $\mu_{11} = r - d_1$, and $\mu_{12} = a_3 - d_2$, therefore the VEP is locally asymptotically stable (LAS) provided that the following conditions are met.

$$r < d_1 \tag{10}$$

$$a_3 < d_2 \tag{11}$$

The JM at the FAEP can be represented by:

$$J_{E_2} = \begin{bmatrix} -bh_1 & -h_1\left(\frac{a_1}{K_1+h_1} + rf\right) \\ 0 & \frac{a_2h_1}{K_1+h_1} + a_3 - d_2 \end{bmatrix}. \tag{12}$$

Hence the eigenvalues are $\mu_{21} = -bh_1 < 0$, and $\mu_{22} = \frac{a_2h_1}{K_1+h_1} + a_3 - d_2$, therefore the FAEP will be LAS provided that the following condition holds.

$$\frac{a_2h_1}{K_1+h_1} + a_3 < d_2. \tag{13}$$

The JM of the system (1) at the SAEP can be written in the form:

$$J_{E_3} = \begin{bmatrix} \frac{r}{1+fh_2} - d_1 - \frac{a_1(1-ch_2)h_2}{K_1} & 0 \\ h_2\frac{a_2(1-ch_2)}{K_1} & -\frac{K_2e(1-m)h_2}{[K_2+(1-m)h_2]^2} \end{bmatrix}. \tag{14}$$

Accordingly, the eigenvalue can be determined as $\mu_{31} = \frac{r}{1+fh_2} - d_1 - \frac{a_1(1-ch_2)h_2}{K_1}$, and $\mu_{32} = -\frac{K_2e(1-m)h_2}{[K_2+(1-m)h_2]^2} < 0$, hence the SAEP will be LAS provided that

$$\frac{r}{1+fh_2} < d_1 + \frac{a_1(1-ch_2)h_2}{K_1}. \tag{15}$$

The JM at the COEP will be written as follows:

$$J_{E_4} = \begin{bmatrix} a_{11} & a_{12} \\ a_{21} & a_{22} \end{bmatrix}, \tag{16}$$

where:

$$a_{11} = X^*\left[\frac{a_1Y^*(1-cY^*)^2}{[K_1+X^*(1-cY^*)]^2} - b\right],$$

$$a_{12} = -X^*\left[\frac{K_1a_1(1-2cY^*)+a_1X^*(1-cY^*)^2}{[K_1+X^*(1-cY^*)]^2} + \frac{rf}{(1+fY^*)^2}\right] < 0,$$

$$a_{21} = Y^*\left[\frac{K_1a_2(1-cY^*)}{[K_1+X^*(1-cY^*)]^2}\right] > 0,$$

$$a_{22} = -Y^*\left[\frac{K_1a_2cX^*}{[K_1+X^*(1-cY^*)]^2} + \frac{K_2e(1-m)}{[K_2+(1-m)Y^*]^2}\right] < 0.$$

Straightforward computation shows that the characteristic equation of J_{E_4} will be written as:

$$\mu^2 - Tr_{E_4}\mu + Det_{E_4} = 0; \tag{17}$$

where $Tr_{E_4} = a_{11} + a_{22}$, and $Det_{E_4} = a_{11}a_{22} - a_{12}a_{21}$.

Clearly, equation (17) has the following roots (eigenvalues):

$$\mu_{41} = \frac{Tr_{E_4} + \sqrt{(Tr_{E_4})^2 - 4Det_{E_4}}}{2}, \quad \mu_{42} = \frac{Tr_{E_4} - \sqrt{(Tr_{E_4})^2 - 4Det_{E_4}}}{2} \tag{18}$$

According to the Routh Hurwitz criterion, the two roots μ_{41} and μ_{42} have negative real parts if and only if $Tr_{E_4} < 0$, and $Det_{E_4} > 0$. Therefore, the COEP will be LAS if and only if the following condition holds:

$$\frac{a_1 Y^*(1-cY^*)^2}{[K_1 + X^*(1-cY^*)]^2} < b. \tag{19}$$

The global dynamic of the system (1) is investigated as shown in the following theorems, by computing the basin of attraction using the method of the Lyapunov function, and the Dulac function with the Poincare-Bendixson theorem.

Theorem 3: If the VEP is LAS then it is a globally asymptotically stable.

Proof: Define the function $L_1 = X + \frac{a_1}{a_2}Y$, which is real valued function defined on the state-space Ω, so that $L_1(0,0) = 0$ while $L_1(X,Y) > 0$ for all $(X,Y) \in \Omega$ and $(X,Y) \neq (0,0)$, hence it is a positive definite function.

$$\frac{dL_1}{dt} = \frac{dX}{dt} + \frac{a_1}{a_2}\frac{dY}{dt} = \frac{rX}{1+fY} - d_1X - bX^2 + \frac{a_1a_3}{a_2}Y - \frac{a_1d_2}{a_2}Y - \frac{a_1}{a_2}\frac{e(1-m)Y^2}{K_2+(1-m)Y}.$$

Therefore, after some calculation it is obtained that:

$$\frac{dL_1}{dt} \leq -(d_1 - r)X - \frac{a_1}{a_2}(d_2 - a_3)Y.$$

Clearly, under the LAS conditions, $\frac{dL_1}{dt}$ is negative definite function. Hence the VEP is a GAS.

Theorem 4: If the FAEP is a LAS then it is a GAS provided that the following sufficient condition is met:

$$\frac{(rfK_1 + a_1)}{K_1}h_1 < \frac{a_1}{a_2}(d_2 - a_3). \tag{20}$$

Proof: Define the function $L_2 = X - h_1 - h_1 \ln\frac{X}{h_1} + \frac{a_1}{a_2}Y$, which is a real valued function defined on the $\Omega_1 = \{(X, Y) \in \mathbb{R}_+^2 : X > 0, Y \geq 0\}$, so that $L_2(h_1, 0) = 0$ while $L_2(X, Y) > 0$ for all $(X, Y) \in \Omega_1$ and $(X, Y) \neq (h_1, 0)$, hence it is a positive definite function.

The derivative of L_2 with respect to time can be written as:

$$\frac{dL_2}{dt} \leq -b(X - h_1)^2 - \left[\frac{a_1}{a_2}(d_2 - a_3) - \frac{(rfK_1 + a_1)}{K_1} h_1\right] Y.$$

Clearly, under the condition (20), $\frac{dL_2}{dt}$ is negative definite function. Hence the FAEP is a GAS.

Theorem 5: If the SAEP is a LAS then it is a GAS provided that the sufficient condition (10) is met

Proof: Define the function $L_3 = \frac{a_2}{a_1} X + Y - h_2 - h_2 \ln \frac{Y}{h_2}$, which is a real valued function defined on the $\Omega_2 = \{(X, Y) \in \mathbb{R}_+^2 : X \geq 0, Y > 0\}$, so that $L_3(0, h_2) = 0$ while $L_3(X, Y) > 0$ for all $(X, Y) \in \Omega_2$ and $(X, Y) \neq (0, h_2)$, hence it is a positive definite function.

The derivative of L_3 with respect to time can be written as:

$$\frac{dL_3}{dt} \leq -\frac{a_2}{a_1}(d_1 - r)X - \frac{e(1-m)K_2(Y-h_2)^2}{[K_2+(1-m)Y][K_2+(1-m)h_2]} - \frac{a_2 X(1-cY)h_2}{K_1 + X(1-cY)}$$

Since $0 < 1 - cY < 1$, then it is obtained that

$$\frac{dL_3}{dt} \leq -\frac{a_2}{a_1}[d_1 - r]X - \frac{e(1-m)K_2(Y-h_2)^2}{[K_2+(1-m)Y][K_2+(1-m)h_2]}.$$

Clearly, under the condition (10), $\frac{dL_3}{dt}$ is negative definite function. Hence the SAEP is a GAS.

Theorem 6: If the COEP is a unique LAS then it is a GAS

Proof: Consider a continuously differentiable function $g(X, Y)$ (known as the Dulac function) such that the expression $\Delta = \frac{\partial}{\partial X}(gG_1) + \frac{\partial}{\partial Y}(gG_2)$ almost everywhere has the same sign $(\neq 0)$ in a simply connected region of the plane. Consequently, according to the Bendixson–Dulac theorem [33], the autonomous dynamical system (1) has no non-constant periodic solutions belonging entirely in the region.

Consider the function $g(X, Y) = \frac{1}{XY}$, which is a C^1 in a simply connected region of Ω, then simple computation shows that:

$$\Delta = \frac{\partial}{\partial X}(gG_1) + \frac{\partial}{\partial Y}(gG_2) = \left[-\frac{b}{Y} + \frac{a_1(1-cY)^2}{[K_1+X(1-cY)]^2}\right] - \left[\frac{a_2 cK_1}{[K_1+X(1-cY)]^2} + \frac{eK_2(1-m)}{X[K_2+(1-m)Y]^2}\right].$$

Since, the LAS condition (19) of COEP, is correct for any value of Y^*, then the condition is correct for any value of Y. Therefore, it is deduced that, $\Delta < 0$.

Thus, the system (1) has no periodic dynamics in the interior of Ω. Consequently, depending on the Poincare-Bendixson theorem the COEP is a GAS.

5. PERSISTENCE

The idea of persistence is explored in this section. In biology, persistence refers to the continued existence of all populations, regardless of their origins. It follows mathematically that the boundary of the non-negative state space does not contain any omega limit points for rigorously positive solutions. Conditions guarantee the system's uniform persistence, according to the following theorem (1).

Theorem 7: The system (1) is uniformly persistence under the following conditions

$$\left.\begin{array}{l} d_1 < r \\ d_2 < a_3 \end{array}\right\}. \tag{21}$$

$$d_2 < \frac{a_2 h_1}{K_1 + h_1} + a_3. \tag{22}$$

$$d_1 + \frac{a_1(1 - c h_2) h_2}{K_1} < \frac{r}{1 + f h_2}. \tag{23}$$

Proof: Consider the function $P(X,Y) = X^p Y^q$, where p, and q are positive constants.

Clearly, $P(X,Y) > 0$ for all $(X,Y) \in \Omega$, and $P(X,Y) = 0$ for all $(X,Y) \in \partial\Omega$, where $\partial\Omega$ represents the boundary of the state-space Ω. Then, $P(X,Y)$ is the said to be persistence function or named average Lyapunov function in the sense of the Gard approach [34]. Now, the Gard approach states that the proof is only conclusive if $\Lambda(X,Y) = \frac{P'(X,Y)}{P(X,Y)}$ is positive for all points (X,Y) that belong to the omega limit sets of the system (1) in the $\partial\Omega$.

Since the result of direct computation yields that:

$$\begin{aligned} \Lambda(X,Y) = \frac{p}{X}\frac{dX}{dt} + \frac{q}{Y}\frac{dY}{dt} = p\left[\frac{r}{1+fY} - d_1 - bX - \frac{a_1(1-cY)Y}{K_1 + X(1-cY)}\right] \\ + q\left[\frac{a_2 X(1-cY)}{K_1 + X(1-cY)} + a_3 - d_2 - \frac{e(1-m)Y}{K_2 + (1-m)Y}\right] \end{aligned}.$$

Moreover, since E_1, E_2, and E_3 are the only possible attracting sets belong to the omega limit sets of the system (1) in $\partial\Omega$. Then, the direct calculation leads to that:

$\Lambda(E_1) = p(r - d_1) + q(a_3 - d_2)$.

$\Lambda(E_2) = q\left(\frac{a_2 h_1}{K_1 + h_1} + a_3 - d_2\right)$.

$\Lambda(E_3) = p\left(\frac{r}{1 + f h_2} - d_1 - \frac{a_1(1 - c h_2) h_2}{K_1}\right)$.

Clearly, under the set of conditions (21) or at least one condition of them with a suitable choice of p and q, it is obtained that $\Lambda(E_1) > 0$. While $\Lambda(E_2) > 0$ due to condition (22). However, condition (23) guarantees that $\Lambda(E_3) > 0$. Hence the proof is done.

6. LOCAL BIFURCATION

The integral curves of a set of vector fields or the solutions to a set of differential equations are two examples of collections of curves that might undergo changes in their qualitative structure according to the bifurcation theory. A bifurcation happens when a small, gradual change in a system's parameter values results in a large qualitative shift in the behavior of the system. The mathematical analysis of dynamical systems is where it is most frequently employed. There are two types of bifurcation. Both local and global bifurcations can be distinguished by looking for changes in the local stability characteristics of equilibria, periodic orbits, or other invariant sets when parameters cross critical thresholds. Global bifurcations take place when the system's larger invariant sets interfere with one another or with the system's equilibria. They can't be discovered just by looking at how stable the equilibria are. This section carries out the detection of the potential for local bifurcation.

Rewrite the system (1) as:

$$\frac{dW}{dt} = G(W, \alpha), \text{ with } W = \begin{pmatrix} X \\ Y \end{pmatrix}, \ \alpha \in \mathbb{R}_+ \text{ and } G(W, \alpha) = \begin{pmatrix} G_1(X, Y, \alpha) \\ G_2(X, Y, \alpha) \end{pmatrix}.$$

Hence, the second directional derivative of G, with $V = (v_1, v_2)^T$ be any vector, can be written using direct computation as:

$$D^2 G(W, \alpha).(V, V) = \begin{pmatrix} c_{11} \\ c_{21} \end{pmatrix}, \tag{24}$$

where

$$c_{11}=-2\left[b-\frac{a_1K_1Y(1-cY)^2}{[K_1+X(1-cY)]^3}\right]{v_1}^2+2X\left[\frac{ca_1K_1(K_1+X)}{[K_1+X(1-cY)]^3}+\frac{rf^2}{(1+fY)^3}\right]{v_2}^2$$
$$+2\left[a_1K_1\left(\frac{c(2K_1+X)Y-(K_1+X)}{[K_1+X(1-cY)]^3}\right)-\frac{rf}{(1+fY)^2}\right]v_1v_2,$$

$$c_{21}=-2\left[\frac{a_2K_1c(K_1+X)X}{[K_1+X(1-cY)]^3}+\frac{eK_2{}^2(1-m)}{[K_2+(1-m)y]^3}\right]{v_2}^2-2a_2K_1\left[\frac{Y-2cY^2+c^2Y^3}{[K_1+X(1-cY)]^3}\right]{v_1}^2$$
$$+2a_2K_1\left[\frac{(K_1+X)-c(2K_1+X)Y}{[K_1+X(1-cY)]^3}\right]v_1v_2.$$

While the third directional derivative of G can be written as:

$$D^3G(W,\alpha).(V,V,V)=\begin{pmatrix}d_{11}\\ d_{21}\end{pmatrix},\qquad(25)$$

where:

$$d_{11}=\frac{6a_1K_1Y(-1+cY)^3}{(X-cXY+K_1)^4}v_1^3+\frac{6a_1K_1(1-cY)[X(1-cY)+(1-3cY)K_1]}{(X-cXY+K_1)^4}v_1^2v_2$$
$$+\left[\frac{6a_1K_1c[X^2(-1+cY)+2cXYK_1+K_1^2]}{(X-cXY+K_1)^4}+\frac{6f^2r(1+fY)}{(1+fY)^4}\right]v_1v_2^2$$
$$+\left[-\frac{6f^3rX}{(1+fY)^4}+\frac{6a_1K_1c^2X^2(X+K_1)}{(X-cXY+K_1)^4}\right]v_2^3.$$
$$d_{21}=\left[\frac{6e(1-m)^2K_2^2}{((1-m)Y+K_2)^4}-\frac{6a_2K_1c^2X^2(X+K_1)}{(X-cXY+K_1)^4}\right]v_2^3+\frac{6a_2K_1Y(1-cY)^3}{(X-cXY+K_1)^4}v_1^3$$
$$-\frac{6a_2K_1(1-cY)[X(1-cY)+(1-3cY)K_1]}{(X-cXY+K_1)^4}v_1^2v_2$$
$$-\frac{6a_2K_1c[-X^2(1-cY)+2cXYK_1+K_1^2]}{(X-cXY+K_1)^4}v_1v_2^2.$$

Theorem 8: Assume that condition (10) holds, then the system (1) possess a transcritical bifurcation (TB) at the VEP when the parameter a_3 passes through the value $a_3^*=d_2$.

Proof: From the JM that is written in equation (9), it is observed that, for $a_3=a_3^*$ it is becomes

$$J_1=J_{E_1,a_3^*}=\begin{bmatrix}r-d_1 & 0\\ 0 & 0\end{bmatrix}.$$

Therefore, the eigenvalues of J_1 are $\mu_{11}^*=r-d_1$, which is negative under condition (10), and $\mu_{12}^*=0$. Thus, the VEP becomes a non-hyperbolic point. Let $V_1=\begin{pmatrix}v_{11}\\ v_{21}\end{pmatrix}$, and $U_1=\begin{pmatrix}u_{11}\\ u_{21}\end{pmatrix}$ be the eigenvectors associated with the $\mu_{12}^*=0$ of the J_1 and its transpose respectively. Then, after doing simple mathematical steps it is deduced that:

$$V_1=\begin{pmatrix}0\\ 1\end{pmatrix},\ U_1=\begin{pmatrix}0\\ 1\end{pmatrix}$$

Moreover, direct computation gives that:

$G_{a_3}(W,a_3)=\begin{pmatrix}0\\Y\end{pmatrix}\Rightarrow G_{a_3}(E_1,a_3^*)=\begin{pmatrix}0\\0\end{pmatrix}$. This gives that $U_1{}^{\mathrm{T}}G_{a_3}(E_1,a_3^*)=0$.

$U_1{}^{\mathrm{T}}\left[DG_{a_3}(E_1,a_3^*)V_1\right]=1\neq 0,$

where $DG_{a_3}(E_1,a_3^*)$ represents the directional derivative of $G_{a_3}(W,a_3)$ at (E_1,a_3^*).

Moreover, from the equation (24), the following finding is obtained

$$D^2G(E_1,a_3^*).(V_1,V_1)=\begin{pmatrix}0\\-2\left[\frac{e(1-m)}{K_2}\right]\end{pmatrix}.$$

Hence, it is simple to verify that $U_1{}^{\mathrm{T}}[D^2G(E_1,a_3^*).(V_1,V_1)]=-2\left[\frac{e(1-m)}{K_2}\right]\neq 0$. Thus the Sotomayor theorem of local bifurcation [33], specifies that the system (1) possess a TB at the E_1, and that completes the proof.

Theorem 9: The system (1) possess a TB at the FAEP when the parameter d_2 passes through the value $d_2^*=\frac{a_2h_1}{K_1+h_1}+a_3$.

Proof: From the JM that is written in equation (12), it is observed that, for $d_2=d_2^*$ it is becomes

$$J_2=J_{E_2,d_2^*}=\begin{bmatrix}-bh_1 & -h_1\left(\frac{a_1}{K_1+h_1}+rf\right)\\ 0 & 0\end{bmatrix}.$$

Hence the eigenvalues are $\mu_{21}^*=-bh_1<0$, and $\mu_{22}^*=0$. Thus, the FAEP becomes a non-hyperbolic point. Let $V_2=\begin{pmatrix}v_{12}\\v_{22}\end{pmatrix}$, and $U_2=\begin{pmatrix}u_{12}\\u_{22}\end{pmatrix}$ be the eigenvectors associated with the $\mu_{22}^*=0$ of the J_2 and its transpose respectively. Then, after doing simple mathematical steps it is deduced that:

$$V_2=\begin{pmatrix}-\frac{1}{b}\left[\frac{a_1}{K_1+h_1}+rf\right]\\1\end{pmatrix}=\begin{pmatrix}\gamma_1\\1\end{pmatrix},\ U_2=\begin{pmatrix}0\\1\end{pmatrix}.$$

Moreover, direct computation gives that:

$G_{d_2}(W,d_2)=\begin{pmatrix}0\\-Y\end{pmatrix}\Rightarrow G_{d_2}(E_2,d_2^*)=\begin{pmatrix}0\\0\end{pmatrix}$. This gives that $U_2{}^{\mathrm{T}}G_{d_2}(E_2,d_2^*)=0$.

$U_2{}^{\mathrm{T}}\left[DG_{d_2}(E_2,d_2^*)V_2\right]=-1\neq 0,$

where $DG_{d_2}(E_2,d_2^*)$ represents the directional derivative of $G_{d_2}(W,d_2)$ at (E_2,d_2^*).

Moreover, from the equation (24), the following finding is obtained

$$D^2G(E_2,d_2^*).(V_2,V_2)=\begin{pmatrix}-2b{\gamma_1}^2+2\left[\frac{ca_1K_1h_1}{[K_1+h_1]^2}+rf^2h_1\right]-2\left[\frac{a_1K_1}{[K_1+h_1]^2}+rf\right]\gamma_1\\ -2\left[\frac{a_2K_1ch_1}{[K_1+h_1]^2}+\frac{e(1-m)}{K_2}\right]+2\left[\frac{a_2K_1}{[K_1+h_1]^2}\right]\gamma_1\end{pmatrix}.$$

Hence, due to that $\gamma_1<0$, it is simple to verify that:

$${U_2}^{\mathrm{T}}[D^2G(E_2,d_2^*).(V_2,V_2)]=-2\left[\frac{a_2K_1ch_1}{[K_1+h_1]^2}+\frac{e(1-m)}{K_2}\right]+2\left[\frac{a_2K_1}{[K_1+h_1]^2}\right]\gamma_1<0.$$

Thus the Sotomayor theorem of local bifurcation, specifies that the system (1) possess a TB at the E_2, and that completes the proof.

Theorem 10: The system (1) possess a TB at the SAEP when the parameter r passes through the value $r^*=(1+fh_2)\left[d_1+\frac{a_1(1-ch_2)h_2}{K_1}\right]$, provided that the following condition is satisfied:

$$-2\left[b-\frac{a_1h_2(1-ch_2)^2}{{K_1}^2}\right]-2\left[a_1\frac{(1-2ch_2)}{K_1}+\frac{r^*f}{(1+fh_2)^2}\right]\gamma_2\neq 0. \quad (26)$$

Otherwise, there is a pitchfork bifurcation (PB).

$$-\frac{6a_1h_2(1-ch_2)^3}{{K_1}^3}+\frac{6a_1(1-ch_2)(1-3ch_2)}{{K_1}^2}\gamma_2+\left[\frac{6a_1c}{K_1}+\frac{6f^2r}{(1+fh_2)^3}\right]\gamma_2^2\neq 0. \quad (27)$$

where all the new symbols are given in the proof.

Proof: From the JM that is written in equation (12), it is observed that, for $d_2=d_2^*$ it is becomes

$$J_3=J_{E_3,r^*}=\begin{bmatrix}0 & 0\\ h_2\frac{a_2(1-ch_2)}{K_1} & -\frac{K_2e(1-m)h_2}{[K_2+(1-m)h_2]^2}\end{bmatrix}.$$

Hence the eigenvalues are $\mu_{31}^*=0$, and $\mu_{32}^*=-\frac{K_2e(1-m)h_2}{[K_2+(1-m)h_2]^2}$. Thus, the SAEP becomes a non-hyperbolic point. Let $V_3=\binom{v_{13}}{v_{23}}$, and $U_3=\binom{u_{13}}{u_{23}}$ be the eigenvectors associated with the $\mu_{31}^*=0$ of the J_3 and its transpose respectively. Then, after doing simple mathematical steps it is deduced that:

$$V_3=\begin{pmatrix}1\\ \frac{a_2(1-ch_2)[K_2+(1-m)h_2]^2}{K_1K_2e(1-m)}\end{pmatrix}=\binom{1}{\gamma_2},\ U_3=\binom{1}{0}.$$

Moreover, direct computation gives that:

$$G_r(W,r)=\begin{pmatrix}\frac{X}{1+fY}\\ 0\end{pmatrix}\Rightarrow G_r(E_3,r^*)=\binom{0}{0}. \text{ This gives that } {U_3}^{\mathrm{T}}G_r(E_3,r^*)=0.$$

$$U_3{}^{\mathrm{T}}[DG_r(E_3,r^*)V_3]=\frac{1}{1+fh_2}\neq 0,$$

where $DG_r(E_3,r^*)$ represents the directional derivative of $G_r(W,r)$ at (E_3,r^*). Moreover, from the equation (24), the following finding is obtained

$$D^2G(E_3,r^*).(V_3,V_3)=\begin{pmatrix}c_{11}(E_3,r^*)\\ c_{21}(E_3,r^*)\end{pmatrix},$$

where

$$c_{11}(E_3,r^*)=-2\left[b-\frac{a_1h_2(1-ch_2)^2}{K_1{}^2}\right]-2\left[a_1\frac{(1-2ch_2)}{K_1}+\frac{r^*f}{(1+fh_2)^2}\right]\gamma_2.$$

$$c_{21}(E_3,r^*)=-2\left[\frac{eK_2{}^2(1-m)}{[K_2+(1-m)h_2]^3}\right]\gamma_2{}^2-2a_2h_2\left[\frac{(ch_2-1)^2}{K_1{}^2}\right]+2a_2\left[\frac{1-2ch_2}{K_1}\right]\gamma_2.$$

Hence, due to condition (26), it is simple to verify that:

$$U_3{}^{\mathrm{T}}[D^2G(E_3,r^*).(V_3,V_3)]=-2\left[b-\frac{a_1h_2(1-ch_2)^2}{K_1{}^2}\right]-2\left[a_1\frac{(1-2ch_2)}{K_1}+\frac{r^*f}{(1+fh_2)^2}\right]\gamma_2\neq 0.$$

Thus the Sotomayor theorem of local bifurcation, specifies that the system (1) possess a TB at the E_3. Now, if condition (26) is violated then by using equation (25) it is obtained that:

$$D^3G(E_3,r^*).(V_3,V_3,V_3)=\begin{pmatrix}d_{11}(E_3,r^*)\\ d_{21}(E_3,r^*)\end{pmatrix},$$

where

$$d_{11}=-\frac{6a_1h_2(1-ch_2)^3}{K_1{}^3}+\frac{6a_1(1-ch_2)(1-3ch_2)}{K_1{}^2}\gamma_2+\left[\frac{6a_1c}{K_1}+\frac{6f^2r}{(1+fh_2)^3}\right]\gamma_2^2.$$

$$d_{21}=\left[\frac{6e(1-m)^2K_2^2}{(K_2+(1-m)h_2)^4}\right]\gamma_2^3+\frac{6a_2h_2(1-ch_2)^3}{K_1{}^3}-\frac{6a_2(1-ch_2)(1-3ch_2)}{K_1{}^2}\gamma_2-\frac{6a_2c}{K_1}\gamma_2^2.$$

Hence, due to condition (27), it is simple to verify that:

$$U_3{}^{\mathrm{T}}[D^3G(E_3,r^*).(V_3,V_3,V_3)]=-\frac{6a_1h_2(1-ch_2)^3}{K_1{}^3}+\frac{6a_1(1-ch_2)(1-3ch_2)}{K_1{}^2}\gamma_2+\left[\frac{6a_1c}{K_1}+\frac{6f^2r}{(1+fh_2)^3}\right]\gamma_2^2\neq 0.$$

Thus the system (1) possess a PB at the E_3, and that completes the proof.

Theorem 11: The system (1) possess a saddle-node bifurcation (SNB) at COEP when the parameter a_2 passes through the value $a_2^*=\frac{[K_1+X^*(1-cY^*)]^2}{K_1Y^*(1-cY^*)}\frac{a_{11}a_{22}}{a_{12}}$, if the following requirements are met.

$$b<\frac{a_1Y^*(1-cY^*)^2}{[K_1+X^*(1-cY^*)]^2}, \tag{28}$$

$$c_{11}(E_4, a_2^*)\gamma_4 + c_{21}(E_4, a_2^*) \neq 0, \qquad (29)$$

where all the new symbols are given in the proof.

Proof: From the JM that is written in equation (16), it is observed that, for $a_2 = a_2^*$ it is becomes

$$J_4 = J_{E_4, a_2^*} = [a_{ij}^*],$$

where $a_{11}^* = a_{11}$, $a_{12}^* = a_{12}$, $a_{21}^* = a_{21}(a_2^*)$, and $a_{22}^* = a_{22}(a_2^*)$. Straightforward computation shows that the determinant of J_4 at $a_2 = a_2^*$ (i.e. Det_{E_4, a_2^*}) is zero. Then J_4 has zero eigenvalue ($\mu_{41}^* = 0$) with the second eigenvalue $\mu_{42}^* = Tr_{E_4, a_2^*}$. Thus, the COEP is a non-hyperbolic point when $a_2 = a_2^*$.

Let $V_4 = \begin{pmatrix} v_{14} \\ v_{24} \end{pmatrix}$, and $U_4 = \begin{pmatrix} u_{14} \\ u_{24} \end{pmatrix}$ be the eigenvectors associated with $\mu_{41}^* = 0$ of the J_4 and their transpose respectively. Then, direct calculation gives that:

$$V_4 = \begin{pmatrix} -\frac{a_{12}^*}{a_{11}^*} \\ 1 \end{pmatrix} = \begin{pmatrix} \gamma_3 \\ 1 \end{pmatrix}, \; U_4 = \begin{pmatrix} -\frac{a_{21}^*}{a_{11}^*} \\ 1 \end{pmatrix} = \begin{pmatrix} \gamma_4 \\ 1 \end{pmatrix}.$$

According to the elements of J_4 and the condition (26), it is observed that $\gamma_3 > 0$, and $\gamma_4 < 0$. Moreover, simple computation gives that:

$$G_{a_2}(W, a_2) = \begin{pmatrix} 0 \\ \frac{XY(1-cY)}{K_1 + X(1-cY)} \end{pmatrix} \Rightarrow G_{a_2}(E_4, a_2^*) = \begin{pmatrix} 0 \\ \frac{X^*Y^*(1-cY^*)}{K_1 + X^*(1-cY^*)} \end{pmatrix}.$$

This gives that $U_4{}^{\mathrm{T}} G_{a_2}(E_4, a_2^*) = \frac{X^*Y^*(1-cY^*)}{K_1 + X^*(1-cY^*)} > 0$. Moreover, from the equation (24), the following finding is obtained

$$D^2G(E_4, a_2^*).(V_4, V_4) = \begin{pmatrix} c_{11}(E_4, a_2^*) \\ c_{21}(E_4, a_2^*) \end{pmatrix},$$

where

$$c_{11}(E_4, a_2^*) = -2\left[b - \frac{a_1K_1Y^*(1-cY^*)^2}{[K_1 + X^*(1-cY^*)]^3}\right]\gamma_3{}^2$$
$$+2\left[\frac{ca_1K_1(K_1+X^*)X^*}{[K_1 + X^*(1-cY^*)]^3} + \frac{rf^2X^*}{(1+fY^*)^3}\right]$$
$$+2\left[\frac{a_1K_1c(2K_1+X^*)Y^* - a_1K_1(K_1+X^*)}{[K_1 + X^*(1-cY^*)]^3} - \frac{rf}{(1+fY^*)^2}\right]\gamma_3,$$

$$c_{21}(E_4,a_2^*)=-2\left[\frac{a_2K_1c(K_1+X^*)X^*}{[K_1+X^*(1-cY^*)]^3}+\frac{eK_2{}^2(1-m)}{[K_2+(1-m)Y^*]^3}\right]$$
$$-2\left[\frac{a_2K_1Y^*(1-cY^*)^2}{[K_1+X^*(1-cY^*)]^3}\right]\gamma_3{}^2$$
$$+2\left[\frac{a_2K_1(K_1+X^*)-a_2K_1c(2K_1+X^*)Y^*}{[K_1+X^*(1-cY^*)]^3}\right]\gamma_3.$$

Hence, by using the condition (27), it is simple to verify that:

$$U_4{}^{\mathrm{T}}[D^2G(E_4,a_2^*).(V_4,V_4)]=c_{11}(E_4,a_2^*)\gamma_4+c_{21}(E_4,a_2^*)\neq 0.$$

Thus the Sotomayor theorem of local bifurcation, specifies that the system (1) possess a SNB at the E_4, and that completes the proof.

7. NUMERICAL SIMULATION

A numerical simulation for system (1) is carried out in this part. The goal is to specify the influence of parameter values on the dynamical behavior of the system (1) and to confirm the analytical result that was obtained. There were two kinds of software used. Mathematica version 12 was used to obtain the system's (1) direction field, while Matlab version R2013a was used to obtain the phase portrait.

The following hypothetical biologically feasible Dataset is used for doing the simulation.

$$\begin{gathered} r=2,\ f=0.2, b=0.2, d_1=0.1, a_1=0.5, \\ c=0.4, K_1=1, K_2=1, a_2=0.25, a_3=0.1, \\ e=0.4, m=0.8, d_2=0.15. \end{gathered} \tag{30}$$

In the event of a bi-stable situation, the system's (1) trajectories are described using both the blue and green colors; in all other cases, just the blue color is utilized. The equilibrium points are shown by the red balls. However, the system's (1) trajectories are described by the motion's direction using the arrows in the direction field.

It is observed that, the system (1) approaches a unique COEP using the Dataset (2), while as the value of r belongs the range $r\geq 4.5$ the system (1) has at least three COEPs in the interior of positive octant two of them are Nodal sink while the other is saddle point and the system undergoes a bi-stable case, see figures 1 and 2 respectively.

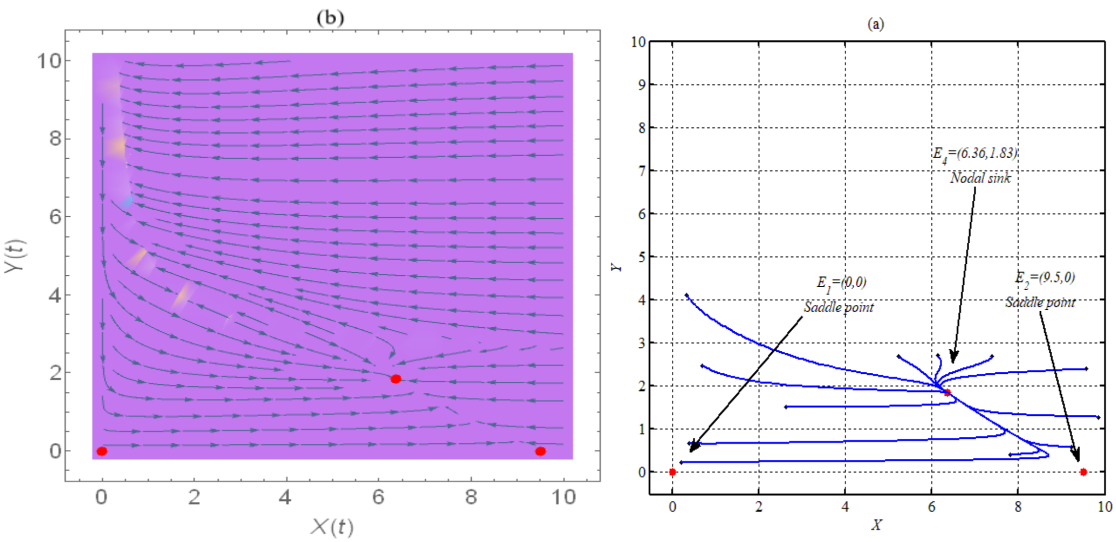

Figure 1: Trajectories of the system (1) utilizing Dataset (30). (a) Phase portrait approaches a COEP. (b) Direction field.

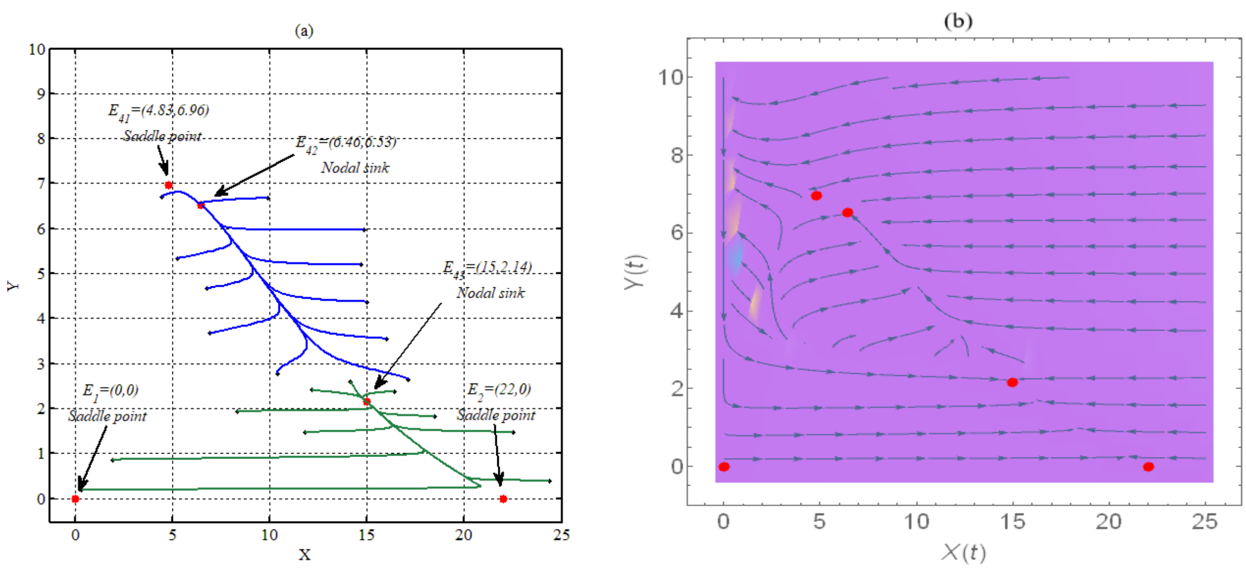

Figure 2: Trajectories of the system (1) utilizing Dataset (30). (a) Phase portrait exhibit bi-stable case between two different COEPs. (b) Direction field.

The influence of the parameter f is shown in figures 3 and 4 using Dataset (30) with $r = 2$ and $r = 4.5$ respectively.

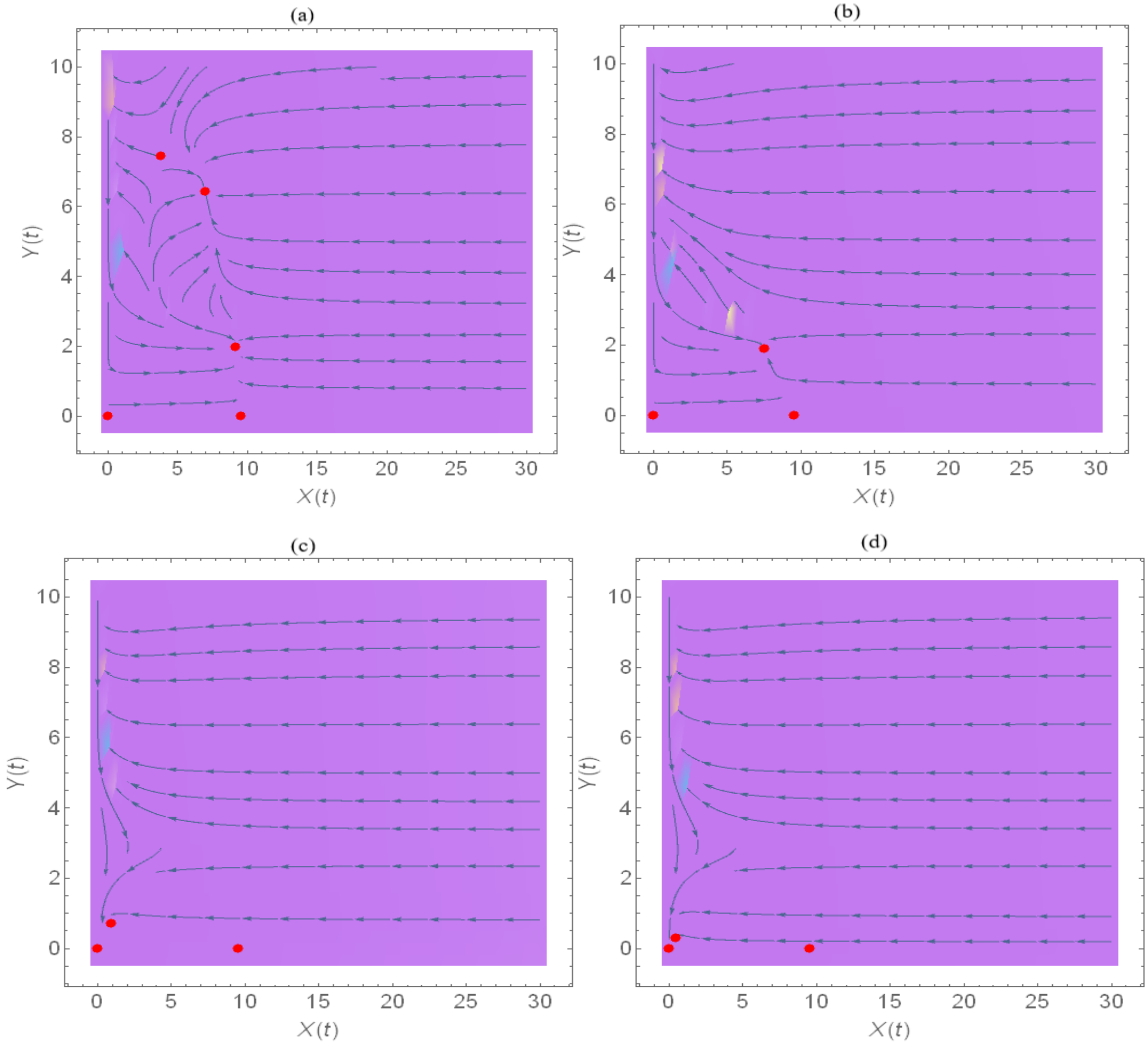

Figure 3: The direction field of the system (1) utilizing the Dataset (30) with different values of f. (a) For $f = 0$, three COEPs are there and the system (1) exhibits a bi-stable case. (b) For $f = 0.1$, the system (1) approaches a COEP. (c) For $f = 5$, the system (1) approaches a COEP. (d) For $f = 20$, the system (1) approaches a COEP.

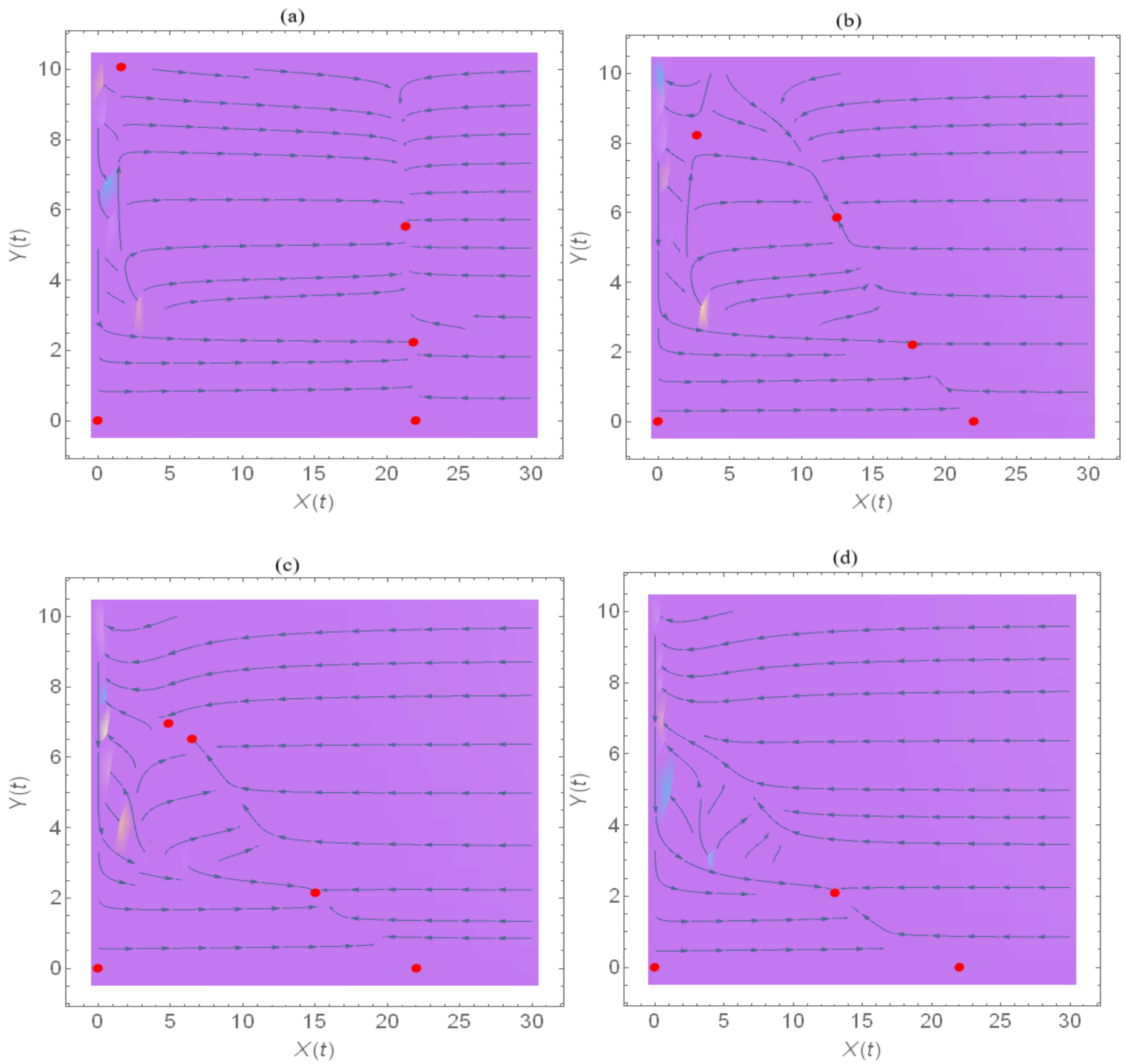

Figure 4: The direction field of the system (1) utilizing the Dataset (30) with $r = 4.5$ and different values of f. (a) For $f = 0$, three COEPs are there and the system (1) exhibits a bi-stable case. (b) For $f = 0.1$, three COEPs are there and the system (1) exhibits a bi-stable case. (c) For $f = 0.2$, three COEPs are there and the system (1) exhibits a bi-stable case. (d) For $f = 0.3$, the system (1) approaches a COEP.

According to figures 3 and 4, it is observed that f has a vital influence on stabilizing the system (1) up to the upper specific value due to reducing the multiplicity of the equilibrium point and transferring the bi-stable case to a stable case. The influence of the parameter b on the system's (1) dynamic is presented in the figure 5.

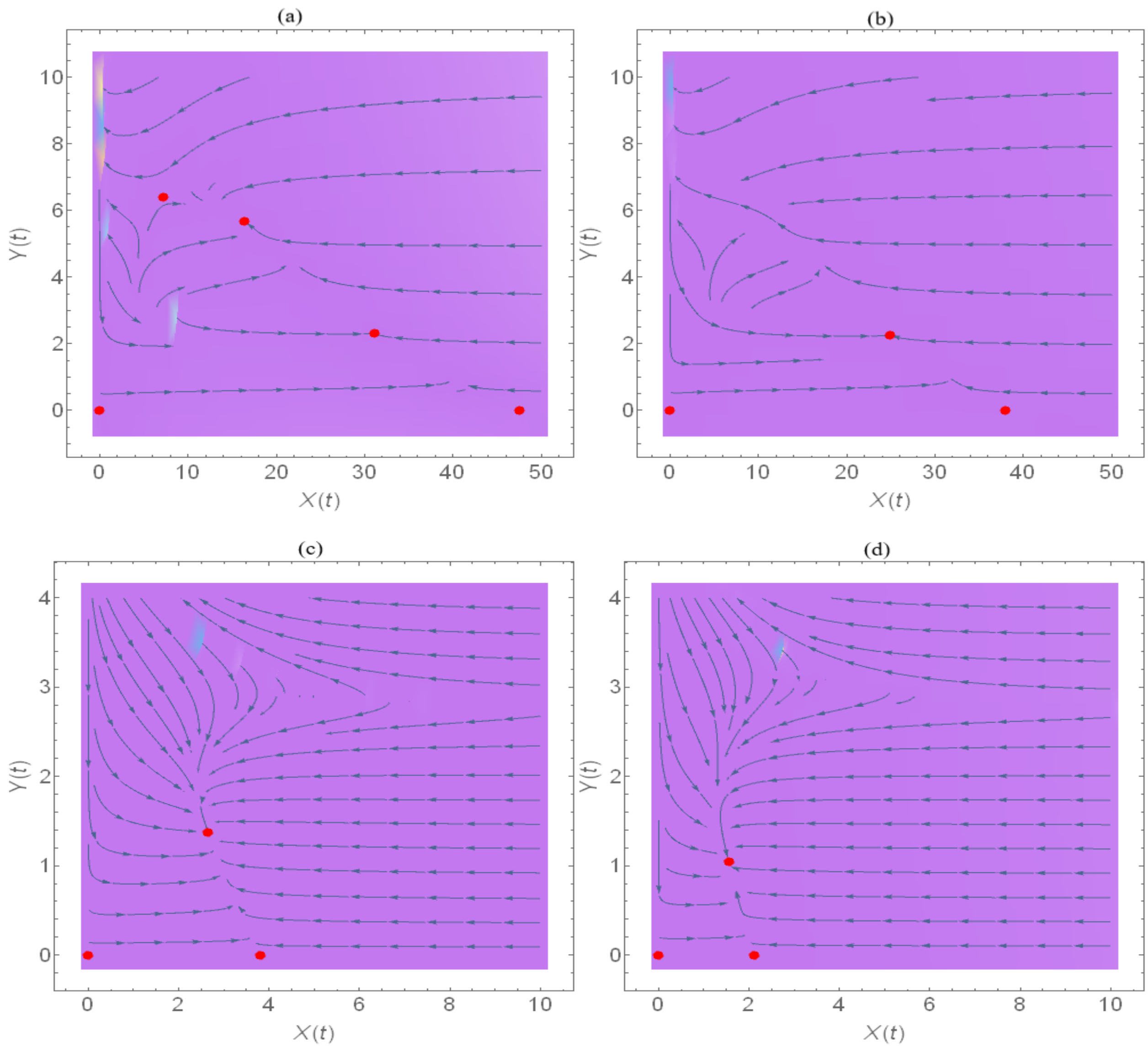

Figure 5: The direction field of the system (1) utilizing the Dataset (30) with different values of b. (a) For $b = 0.04,$ three COEPs are there and the system (1) exhibits a bi-stable case. (b) For $b = 0.05$, the system (1) approaches a COEP. (c) For $b = 0.5$, the system (1) approaches a COEP. (d) For $b = 0.9$, the system (1) approaches a COEP.

It is clear from Figure (5) that parameter b reduces the COEP multiplicity. Furthermore, COEP and FAEP gradually converge to the origin, which means that the population size of both prey and predator decreases simultaneously.

It is observed that the influence of the parameters d_1, a_1, and K_1 on the dynamic of the system (1) is similar to the influence of b. Now, the influence of the parameter c on the dynamic of the system (1) is shown the figure 6 and 7 using Dataset (30) with $r = 2$ and $r = 4.5$ respectively.

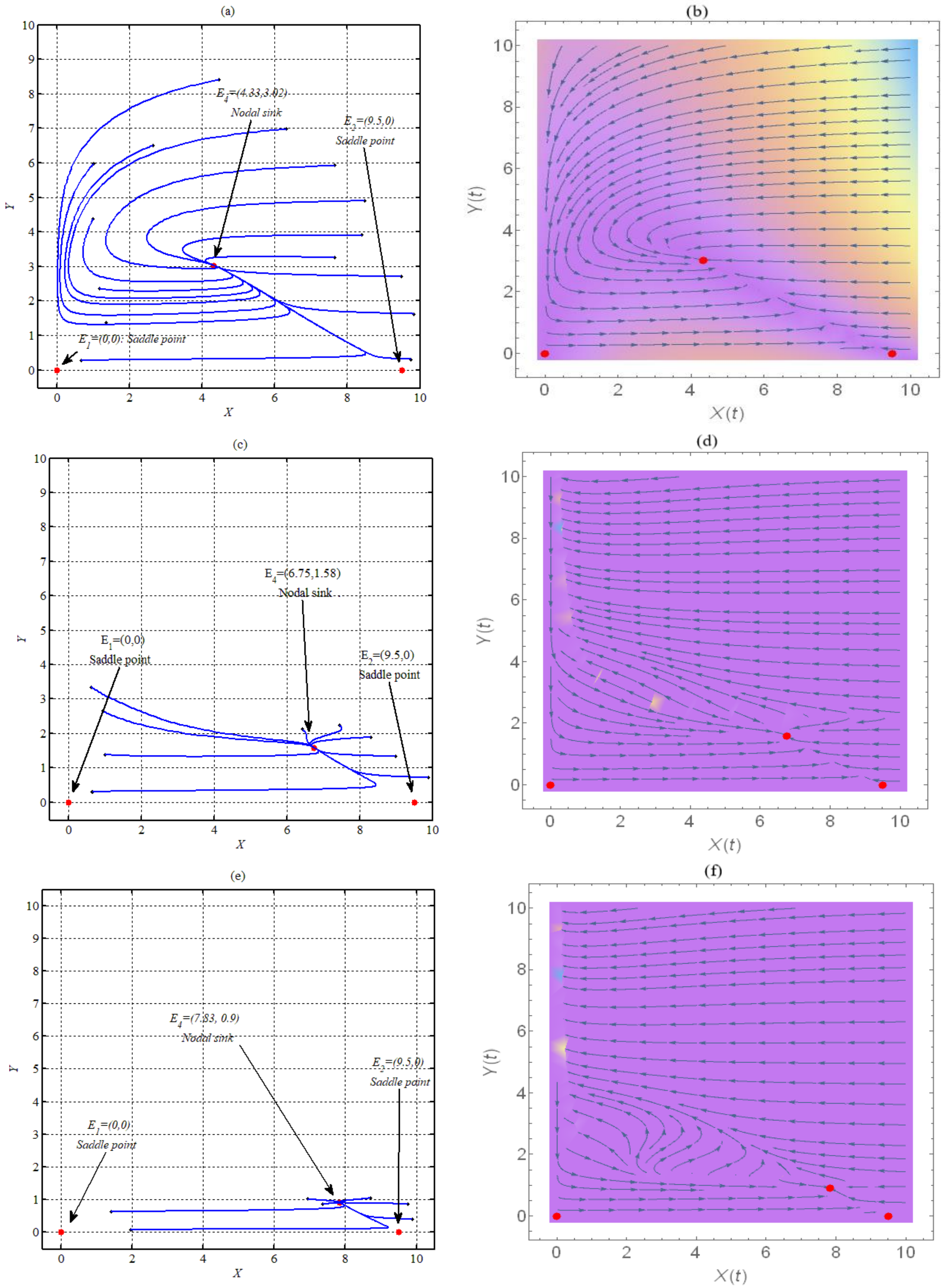

Figure 6: Trajectories of the system (1) utilizing Dataset (30). (a) Phase portrait approaches a COEP when $c = 0.02$. (b) Direction field for $c = 0.02$. (c) Phase portrait approaches a COEP when $c = 0.5$. (d) Direction field for $c = 0.5$. (e) Phase portrait approaches a COEP when $c = 0.99$. (f) Direction field for $c = 0.99$.

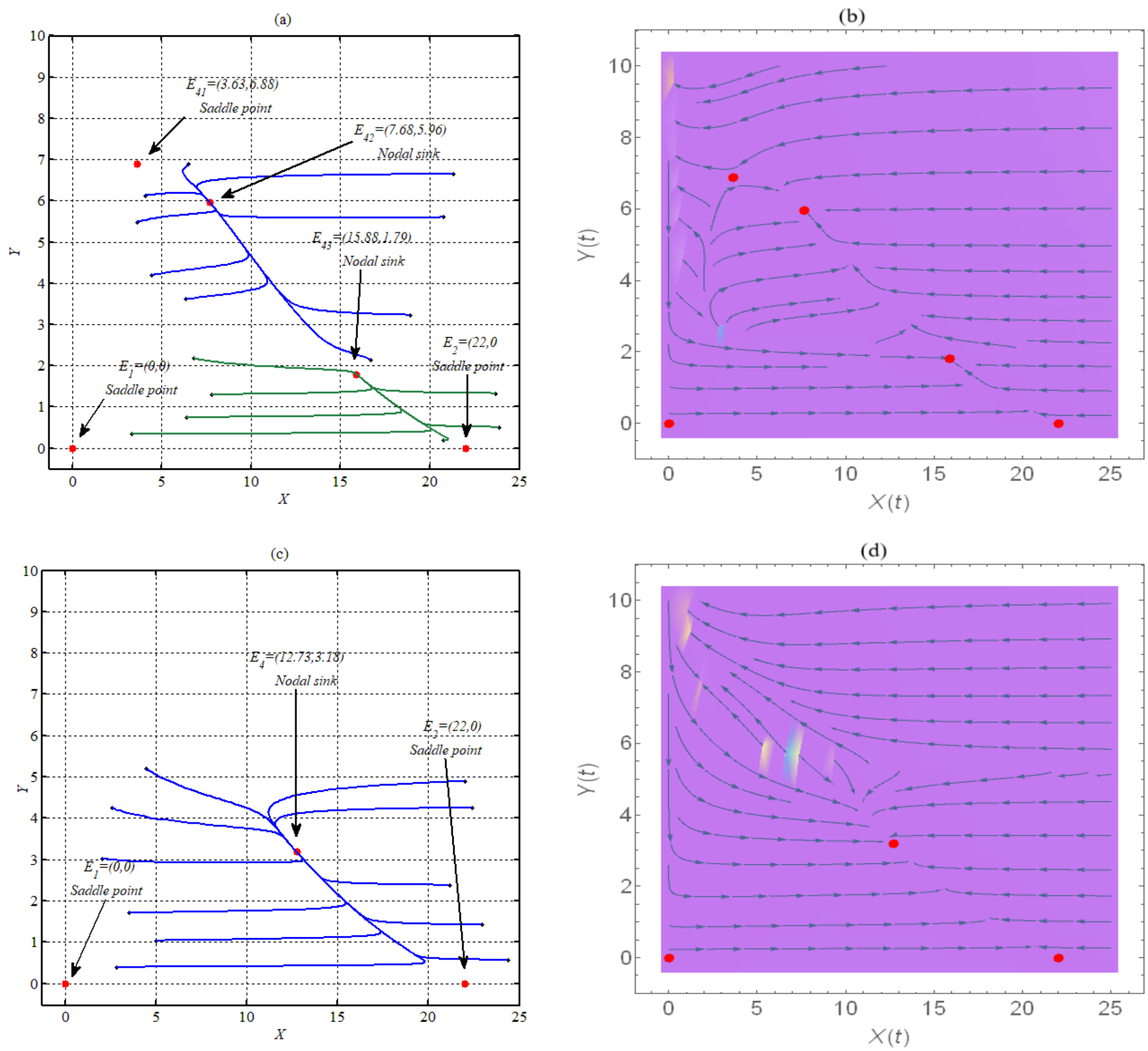

Figure 7: Trajectories of the system (1) utilizing Dataset (30) with $r = 4.5$. (a) Phase portrait exhibit bi-stable case between two different COEPs when $c = 0.5$. (b) Direction field for $c = 0.5$. (c) Phase portrait approaches a COEP when $c = 0.2$. (d) Direction field for $c = 0.2$.

According to Figures 6 and 7, parameter c has a destabilizing influence on the system's (1) dynamics either due to the gradually convergent of a unique COEP to the FAEP, which leads to depletion or extinction in predators or due to the birth of multiple COEPs and bi-stable case occurs. Now, the influence of the parameter a_2 on the dynamic of the system (1) is shown the figure 8 and 9 using Dataset (30) with $r = 2$ and $r = 4.5$ respectively.

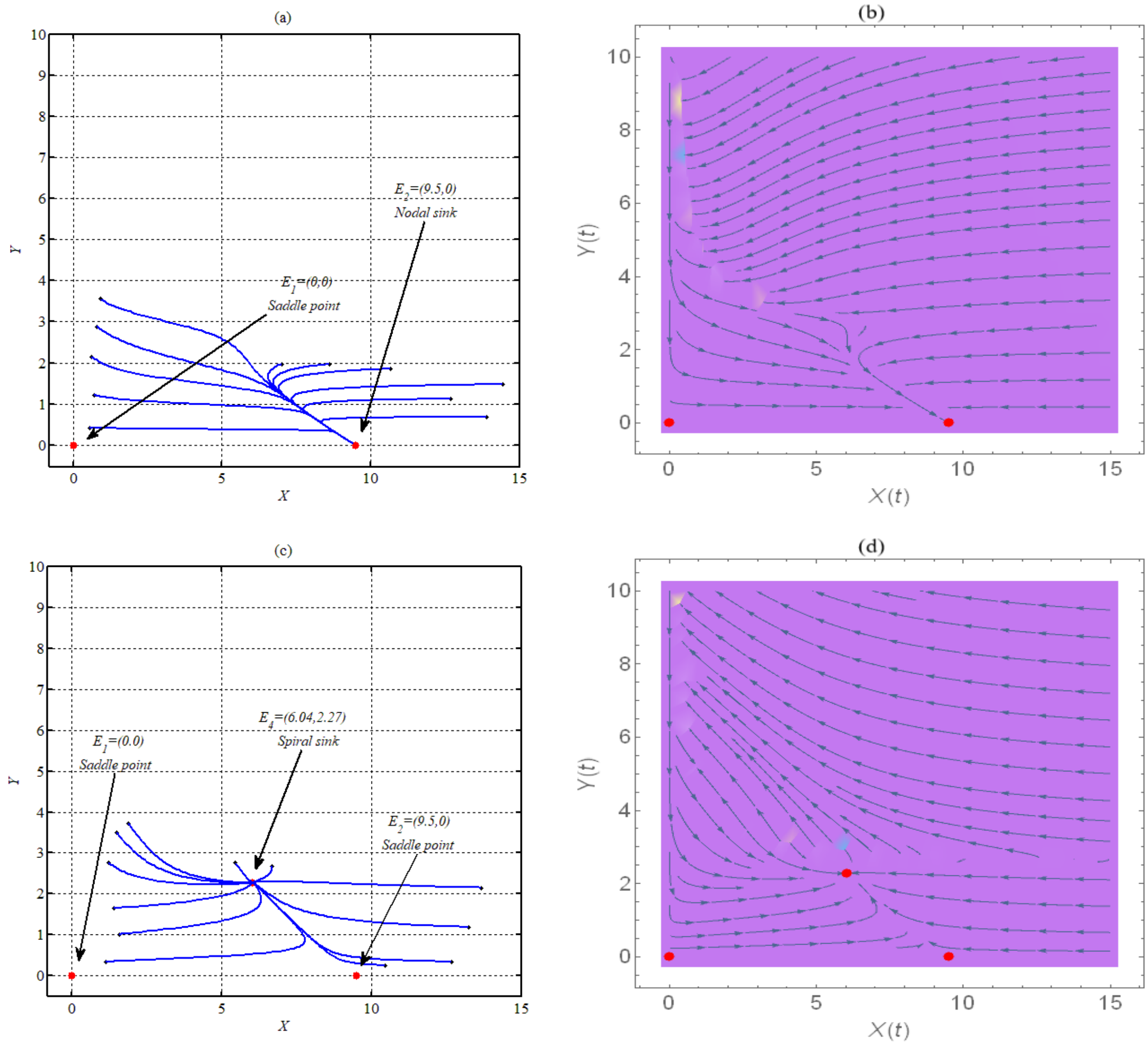

Figure 8: Trajectories of the system (1) utilizing Dataset (30). (a) Phase portrait approaches FAEP when $a_2 = 0.03$. (b) Direction field for $a_2 = 0.03$. (c) Phase portrait approaches a COEP when $a_2 = 0.5$. (d) Direction field for $a_2 = 0.5$.

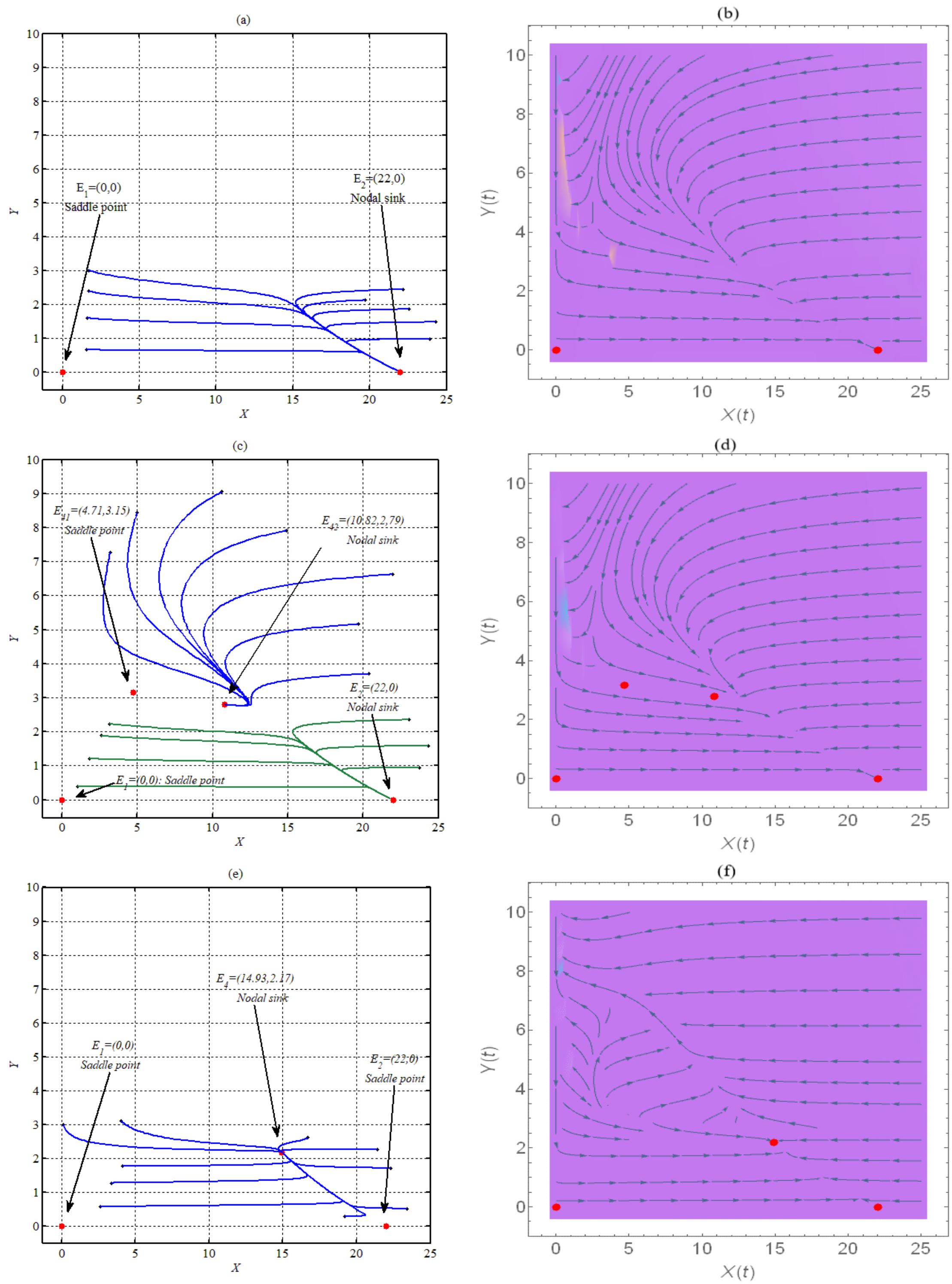

Figure 9: Trajectories of the system (1) utilizing Dataset (30) with $r = 4.5$. (a) Phase portrait approaches FAEP when $a_2 = 0.03$. (b) Direction field for $a_2 = 0.03$. (c) Phase portrait exhibit a bi-stable case between one of the COEPs and the FAEP when $a_2 = 0.04$. (d) Direction field for $a_2 = 0.04$. (e) Phase portrait approaches a COEP when $a_2 = 0.26$. (d) Direction field for $a_2 = 0.26$.

According to figures 8 and 9, the parameter a_2 positively influences the system's persistence (1) and stability. Furthermore, the influence of the parameter a_3 on the dynamic of the system (1) was also studied and explored in figures 10 and 11 using the Dataset (30) with $r = 2$ and $r = 4.5$ respectively.

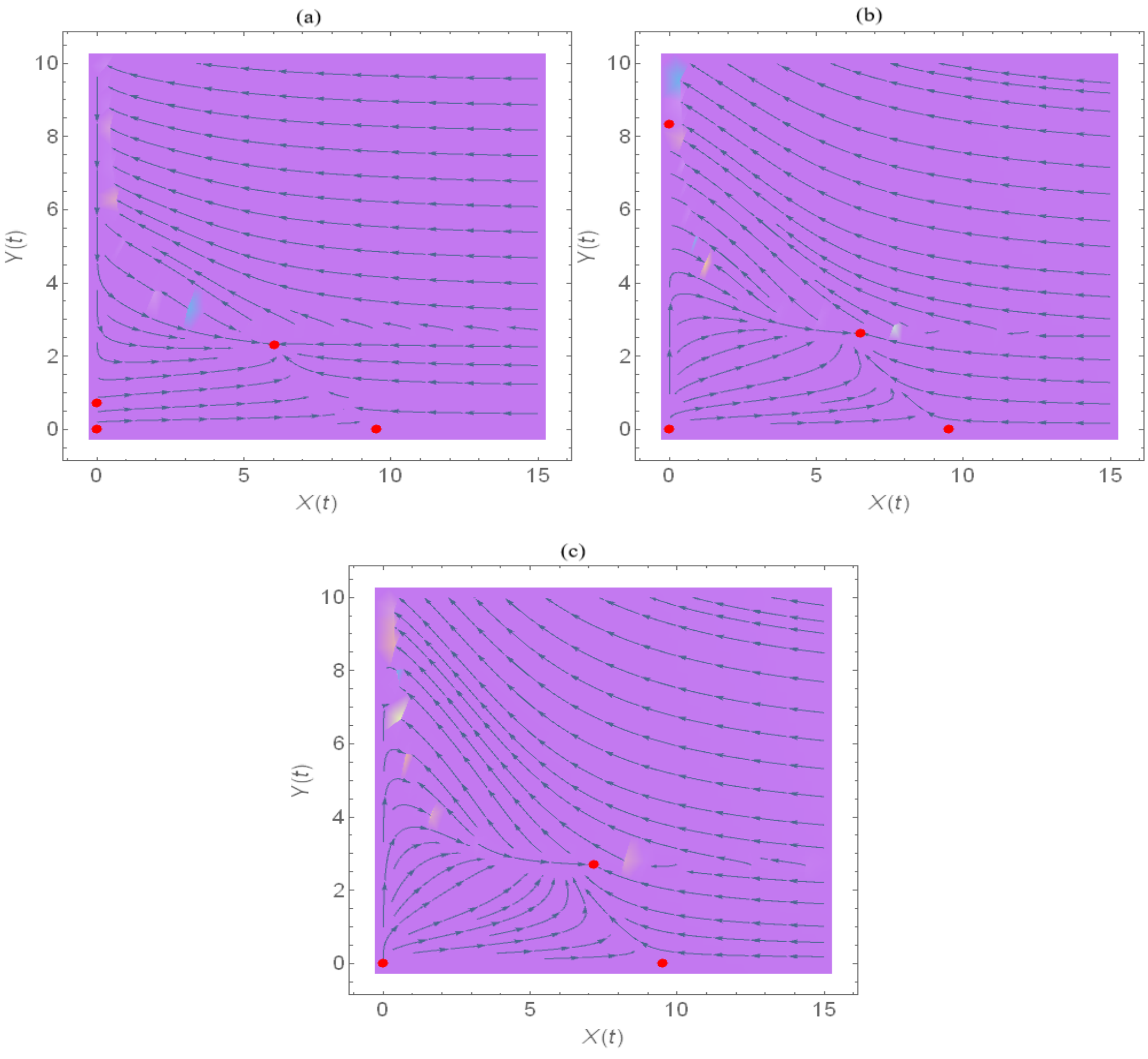

Figure 10: The direction field of the system (1) utilizing the Dataset (30) with different values of a_3. (a) For $a_3 = 0.2$, the system (1) approaches a COEP; the VEP is a nodal source; FAEP and SAEP are saddle points. (b) For $a_3 = 0.4$, the system (1) approaches a COEP; the VEP is a nodal source; FAEP and SAEP are saddle points. (c) For $a_3 = 0.6$, the system (1) approaches a COEP; the VEP is a nodal source; FAEP are saddle points.

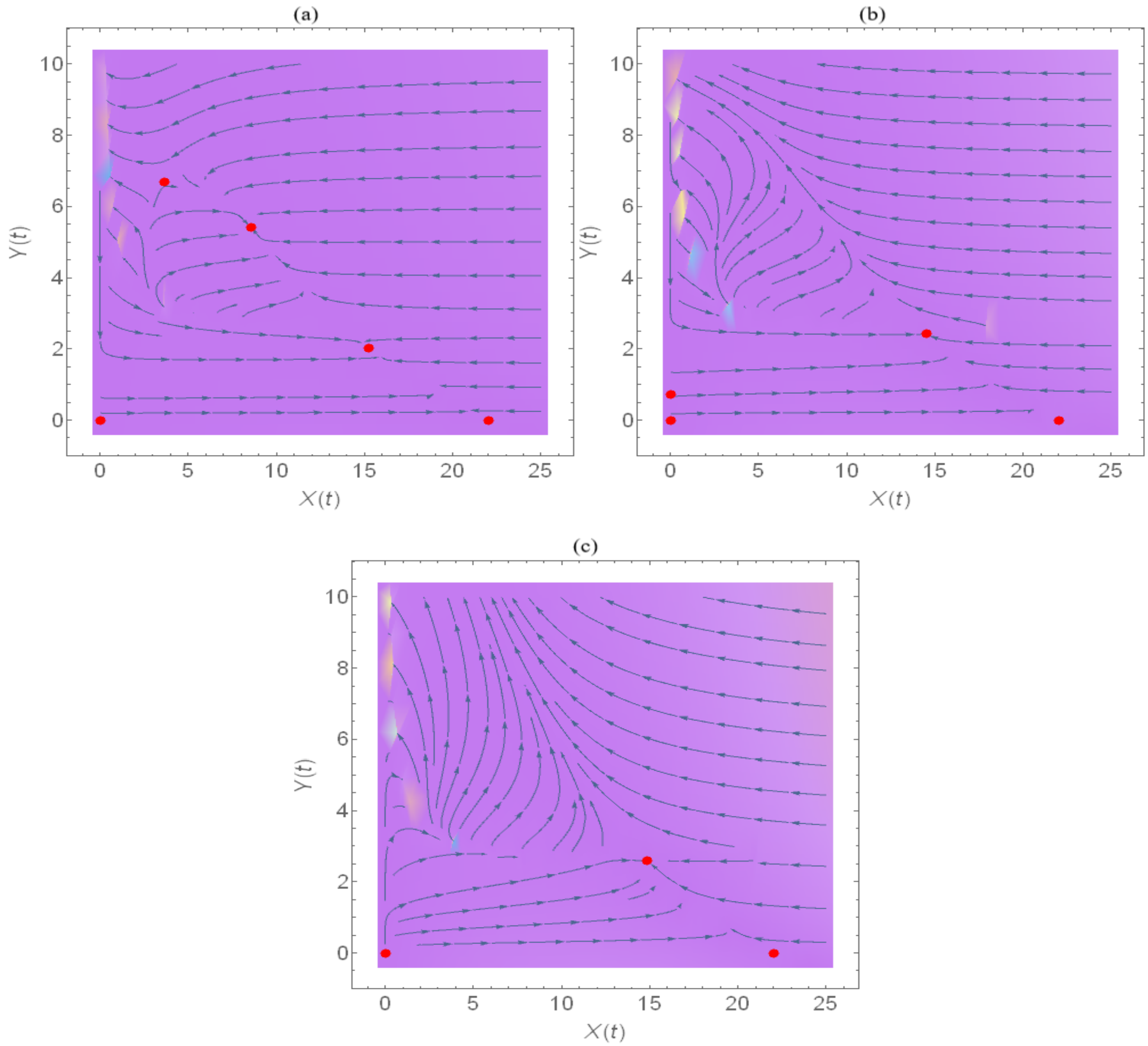

Figure 11: The direction field of the system (1) utilizing the Dataset (30) with $r = 4.5$ and different values of a_3. (a) For $a_3 = 0.08$, three COEPs are there and the system (1) exhibits a bi-stable case; the VEP is a nodal source; FAEP is a saddle point. (b) For $a_3 = 0.2$, the system (1) approaches a COEP; the VEP is a nodal source; FAEP and SAEP are saddle points. (c) For $a_3 = 0.6$, the system (1) approaches a COEP; the VEP is a nodal source; FAEP is a saddle point.

From figures 10 and 11, the SAEP appears when condition (3) is verified and behaves as a saddle point, while it disappears otherwise. Also, these figures show clearly that, the parameter a_3 positively influences the system's persistence (1) and stability.

Figures 12 and 13 show the influence of the parameter d_2 on the dynamic of the system (1) using the Dataset (30) with $r = 2$ and $r = 4.5$ respectively.

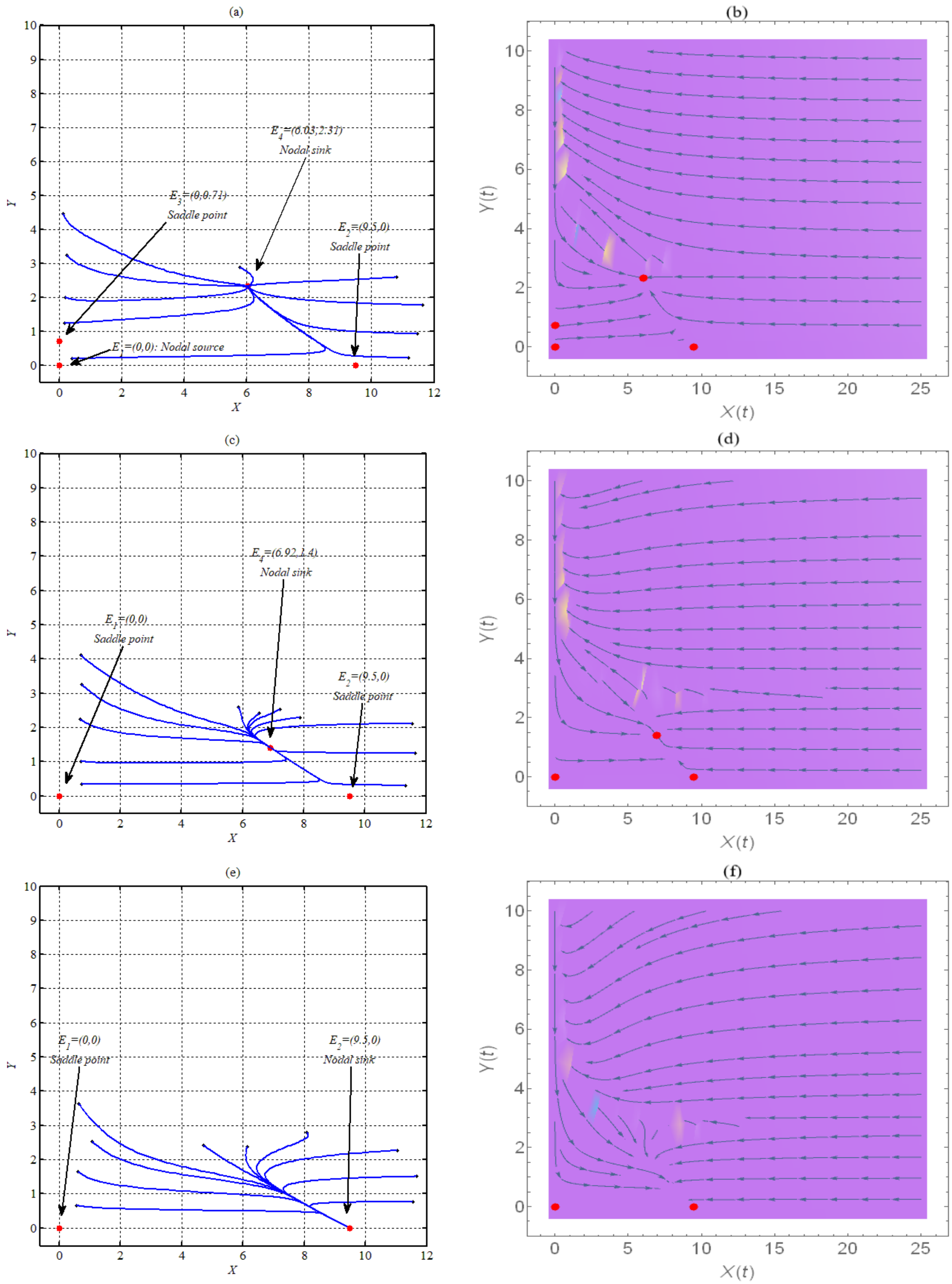

Figure 12: Trajectories of the system (1) utilizing Dataset (30). (a) For $d_2 = 0.05$, phase portrait contains asymptotic stable COEP; Nodal source VEP; FAEP and SAEP are saddle points. (b) Direction field for $d_2 = 0.05$. (c) For $d_2 = 0.2$, phase portrait contains asymptotic stable COEP; VEP and FAEP are saddle points. (d) Direction field for $d_2 = 0.2$. (e) For $d_2 = 0.34$, phase portrait contains asymptotic stable FAEP; VEP is a saddle point. (d) Direction field for $d_2 = 0.34$.

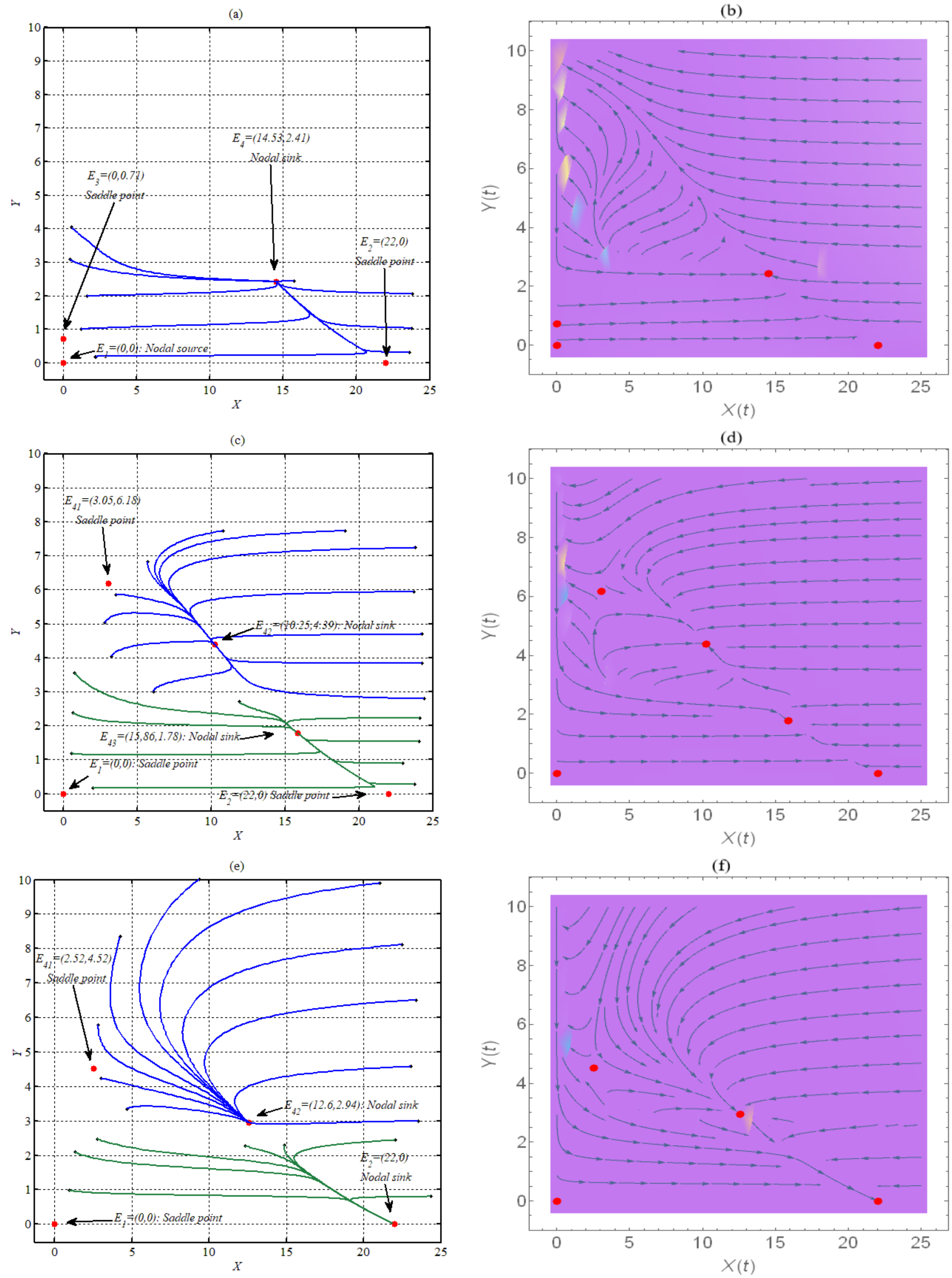

Figure 13: Trajectories of the system (1) utilizing Dataset (30) with $r = 4.5$. (a) For $d_2 = 0.05$, phase portrait contains asymptotic stable COEP; Nodal source VEP; FAEP and SAEP are saddle points. (b) Direction field for $d_2 = 0.05$. (c) For $d_2 = 0.2$, phase portrait contains a bi-stable case between two of the COEPs; VEP, FAEP, and the third COEP are saddle points. (d) Direction field for $d_2 = 0.2$. (e) For $d_2 = 0.4$, phase portrait contains bi-stable case between bi-stable case

between one of the COEPs and the FAEP; VEP, and the second COEP are saddle points. (d) Direction field for $d_2 = 0.4$.

Figures 12 and 13 exhibit destabilizing influence for the parameter d_2, either through the extinction of the predator or else exhibiting a bi-stable behavior.

Finally, our simulation investigation shows that the parameter e has a similar impact on the system's (1) dynamic as that explored with varying c. However, the impact of the parameters m and K_2 is similar to that obtained with varying the parameter a_2.

8. DISCUSSION

Using a combination of predator cannibalism, predation fear, constant predator refuge, and predator-dependent refuge, a Holling type II prey-predator system is developed in this work. The discussion covers every solution property. Both locally and globally, long-term stability behavior is carried out. The system has either a single COEP or multiple points, with a maximum of three boundary equilibrium points. The system is seen to approach the COEP globally if it is unique, but when there are several points, the system exhibits a bi-stable instance. System (1) was also shown to be conditionally persistent; under some circumstances, it experiences TB at the VEP and FAEP, on the other hand, it experiences either TB or PB at the SAEP, depending on the circumstances. Finally, if certain conditions are met, it has an SNB at the COEP. Numerous numerical simulations have been run to illustrate the system's overall dynamics and make it clear how each parameter value affects the dynamics of the suggested system.

9. CONCLUSION

According to the above theoretical and numerical study, the following main conclusions can be reached. There may be several coexistence equilibrium points in the system, which would result in bi-stable behavior. The number of equilibria is decreased when there is a fear rate. The system is stabilized (1) up to the top critical value; after that value, the system faces extinction from predators. It changes the bi-stable state into a stable situation. The intraspecific competition of the prey population, the mortality rate of prey, the maximum attack rate of the predator, and the predator's half-saturation constant all have an adverse effect on the persistence of the populations throughout the entire system. The dynamics of the system are destabilized by the prey's rate of refuge and the predator's rate of cannibalism. The system's persistence (1) and stability have been positively impacted by the rates at which prey and cannibalism biomass is converted into predator birth. Last but not least, the predator's natural mortality rate destabilizes the system (1).

APPENDIX A

The coefficients of the polynomial that given in equation (5) are determined using Mathmatica as:

$$\begin{aligned}\Delta_2= c(1-m)a_1[&-ce^2(1-m)+2e^2f(1-m)+2ce(1-m)a_2-4ef(1-m)a_2-c(1-m)a_2^2\\&+2f(1-m)a_2^2+2ce(1-m)a_3-4ef(1-m)a_3-2c(1-m)a_2a_3+4f(1-m)a_2a_3\\&-c(1-m)a_3^2+2f(1-m)a_3^2-2ce(1-m)d_2+4ef(1-m)d_2+2c(1-m)a_2d_2\\&-4f(1-m)a_2d_2+2c(1-m)a_3d_2-4f(1-m)a_3d_2-c(1-m)d_2^2++2f(1-m)d_2^2\\&+2cefa_2K_2-2cfa_2^2K_2+2cefa_3K_2-4cfa_2a_3K_2-2cfa_3^2K_2\\&-2cefd_2K_2+4c^2fa_2d_2K_2+4cfa_3d_2K_2-2cfd_2^2K_2]\end{aligned}$$

$$\begin{aligned}\Delta_3= &-e^2(1-m)^2a_1+2e(1-m)^2a_1a_2-(1-m)^2a_1a_2^2+2e(1-m)^2a_1a_3\\&-2(1-m)^2a_1a_2a_3-(1-m)^2a_1a_3^2-2e(1-m)^2a_1d_2+2(1-m)^2a_1a_2d_2\\&+2(1-m)^2a_1a_3d_2-(1-m)^2a_1d_2^2+ce(1-m)^2ra_2K_1-c(1-m)^2ra_2^2K_1\\&-c(1-m)^2ra_2a_3K_1-ce(1-m)^2a_2d_1K_1+ef(1-m)^2a_2d_1K_1\\&+c(1-m)^2a_2^2d_1K_1-f(1-m)^2a_2^2d_1K_1+c(1-m)^2a_2a_3d_1K_1\\&-f(1-m)^2a_2a_3d_1K_1+c(1-m)^2ra_2d_2K_1-c(1-m)^2a_2d_1d_2K_1\\&+f(1-m)^2a_2d_1d_2K_1-bef(1-m)^2a_2K_1^2+bf(1-m)^2a_2a_3K_1^2\\&-bf(1-m)^2a_2d_2K_1^2-4ce(1-m)a_1a_2K_2+2ef(1-m)a_1a_2K_2\\&+4c(1-m)a_1a_2^2K_2-2f(1-m)a_1a_2^2K_2-4ce(1-m)a_1a_3K_2\\&+2ef(1-m)a_1a_3K_2+8c(1-m)a_1a_2a_3K_2-4f(1-m)a_1a_2a_3K_2\\&+4c(1-m)a_1a_3^2K_2-2f(1-m)a_1a_3^2K_2+4ce(1-m)a_1d_2K_2\\&-2ef(1-m)a_1d_2K_2-8c(1-m)a_1a_2d_2K_2+4f(1-m)a_1a_2d_2K_2\\&-8c(1-m)a_1a_3d_2K_2+4f(1-m)a_1a_3d_2K_2+4c(1-m)a_1d_2^2K_2\\&-2f(1-m)a_1d_2^2K_2-cef(1-m)a_2d_1K_1K_2+2cf(1-m)a_2^2d_1K_1K_2\\&+2cf(1-m)a_2a_3d_1K_1K_2-2cf(1-m)a_2d_1d_2K_1K_2-c^2a_1a_2^2K_2^2\\&+2cfa_1a_2^2K_2^2-2c^2a_1a_2a_3K_2^2+4cfa_1a_2a_3K_2^2-c^2a_1a_3^2K_2^2+2cfa_1a_3^2K_2^2\\&+2c^2a_1a_2d_2K_2^2-4cfa_1a_2d_2K_2^2+2c^2a_1a_3d_2K_2^2\\&-4cfa_1a_3d_2K_2^2-c^2a_1d_2^2K_2^2+2cfa_1d_2^2K_2^2\end{aligned}$$

$$\Delta_4 = 2ce^2(1-m)^2a_1 - e^2f(1-m)^2a_1 - 4ce(1-m)^2a_1a_2 + 2ef(1-m)^2a_1a_2 + 2c(1-m)^2a_1a_2^2 - f(1-m)^2a_1a_2^2 - 4ce(1-m)^2a_1a_3 + 2ef(1-m)^2a_1a_3 + 4c(1-m)^2a_1a_2a_3 - 2f(1-m)^2a_1a_2a_3 + 2c(1-m)^2a_1a_3^2 - f(1-m)^2a_1a_3^2 + 4ce(1-m)^2a_1d_2 - 2ef(1-m)^2a_1d_2 - 4c(1-m)^2a_1a_2d_2 + 2f(1-m)^2a_1a_2d_2 - 4c(1-m)^2a_1a_3d_2 + 2f(1-m)^2a_1a_3d_2 + 2c(1-m)^2a_1d_2^2 - f(1-m)^2a_1d_2^2 - cef(1-m)^2a_2d_1K_1 + cf(1-m)^2a_2^2d_1K_1 + cf(1-m)^2a_2a_3d_1K_1 - cf(1-m)^2a_2d_1d_2K_1 + 2c^2e(1-m)a_1a_2K_2 - 4cef(1-m)a_1a_2K_2 - 2c^2(1-m)a_1a_2^2K_2 + 4cf(1-m)a_1a_2^2K_2 + 2c^2e(1-m)a_1a_3K_2 - 4cef(1-m)a_1a_3K_2 - 4c^2(1-m)a_1a_2a_3K_2 + 8cf(1-m)a_1a_2a_3K_2 - 2c^2(1-m)a_1a_3^2K_2 + 4cf(1-m)a_1a_3^2K_2 - 2c^2e(1-m)a_1d_2K_2 + 4cef(1-m)a_1d_2K_2 + 4c^2(1-m)a_1a_2d_2K_2 - 8cf(1-m)a_1a_2d_2K_2 + 4c^2(1-m)a_1a_3d_2K_2 - 8cf(1-m)a_1a_3d_2K_2 - 2c^2(1-m)a_1d_2^2K_2 + 4cf(1-m)a_1d_2^2K_2 - c^2fa_1a_2^2K_2^2 - 2c^2fa_1a_2a_3K_2^2 - c^2fa_1a_3^2K_2^2 + 2c^2fa_1a_2d_2K_2^2 + 2c^2fa_1a_3d_2K_2^2 - c^2fa_1d_2^2K_2^2.$$

$$\Delta_5 = -e(1-m)^2ra_2K_1 + (1-m)^2ra_2^2K_1 + (1-m)^2ra_2a_3K_1 + e(1-m)^2a_2d_1K_1 - (1-m)^2a_2^2d_1K_1 - (1-m)^2a_2a_3d_1K_1 - (1-m)^2ra_2d_2K_1 + (1-m)^2a_2d_1d_2K_1 - be(1-m)^2a_2K_1^2 + b(1-m)^2a_2a_3K_1^2 - b(1-m)^2a_2d_2K_1^2 + 2e(1-m)a_1a_2K_2 - 2(1-m)a_1a_2^2K_2 + 2e(1-m)a_1a_3K_2 - 4(1-m)a_1a_2a_3K_2 - 2(1-m)a_1a_3^2K_2 - 2e(1-m)a_1d_2K_2 + 4(1-m)a_1a_2d_2K_2 + 4(1-m)a_1a_3d_2K_2 - 2(1-m)a_1d_2^2K_2 + ce(1-m)ra_2K_1K_2 - 2c(1-m)ra_2^2K_1K_2 - 2c(1-m)ra_2a_3K_1K_2 - ce(1-m)a_2d_1K_1K_2 + ef(1-m)a_2d_1K_1K_2 + 2c(1-m)a_2^2d_1K_1K_2 - 2f(1-m)a_2^2d_1K_1K_2 + 2c(1-m)a_2a_3d_1K_1K_2 - 2f(1-m)a_2a_3d_1K_1K_2 + 2c(1-m)ra_2d_2K_1K_2 - 2c(1-m)a_2d_1d_2K_1K_2 + 2f(1-m)a_2d_1d_2K_1K_2 - bef(1-m)a_2K_1^2K_2 + 2bf(1-m)a_2a_3K_1^2K_2 - 2bf(1-m)a_2d_2K_1^2K_2 + 2ca_1a_2^2K_2^2 - fa_1a_2^2K_2^2 + 4ca_1a_2a_3K_2^2 - 2fa_1a_2a_3K_2^2 + 2ca_1a_3^2K_2^2 - fa_1a_3^2K_2^2 - 4ca_1a_2d_2K_2^2 + 2fa_1a_2d_2K_2^2 - 4ca_1a_3d_2K_2^2 + 2fa_1a_3d_2K_2^2 + 2ca_1d_2^2K_2^2 - fa_1d_2^2K_2^2 + cfa_2^2d_1K_1K_2^2 + cfa_2a_3d_1K_1K_2^2 - cfa_2d_1d_2K_1K_2^2.$$

$$\Delta_6 = -e(1-m)ra_2K_1K_2 + 2(1-m)ra_2^2K_1K_2 + 2(1-m)ra_2a_3K_1K_2 + e(1-m)a_2d_1K_1K_2 - 2(1-m)a_2^2d_1K_1K_2 - 2(1-m)a_2a_3d_1K_1K_2 - 2(1-m)ra_2d_2K_1K_2 + 2(1-m)a_2d_1d_2K_1K_2 - be(1-m)a_2K_1^2K_2 + 2b(1-m)a_2a_3K_1^2K_2 - 2b(1-m)a_2d_2K_1^2K_2 - a_1a_2^2K_2^2 - 2a_1a_2a_3K_2^2 - a_1a_3^2K_2^2 + 2a_1a_2d_2K_2^2 + 2a_1a_3d_2K_2^2 - a_1d_2^2K_2^2 - cra_2^2K_1K_2^2 - cra_2a_3K_1K_2^2 + ca_2^2d_1K_1K_2^2 - fa_2^2d_1K_1K_2^2 + ca_2a_3d_1K_1K_2^2 - fa_2a_3d_1K_1K_2^2 + cra_2d_2K_1K_2^2 - ca_2d_1d_2K_1K_2^2 + fa_2d_1d_2K_1K_2^2 + bfa_2a_3K_1^2K_2^2 - bfa_2d_2K_1^2K_2^2.$$

CONFLICT OF INTERESTS

The author(s) declare that there is no conflict of interest.

REFERENCES

[1] J. Hofbauer, K. Sigmund, Evolutionary games and population dynamics, Cambridge University Press, Cambridge, 1998.

[2] J.D. Murray, Mathematical biology, second ed., Springer, Heidelberg, 1993.

[3] H.I. Freedman, Deterministic mathematical models in population ecology, Marcel Dekker, New York, 1980.

[4] Y. Takeuchi, Global dynamical properties of Lotka–Volterra systems, World Scientific, Singapore, 1996.

[5] M. Haque, M.S. Rahman, E. Venturino, et al. Effect of a functional response-dependent prey refuge in a predator–prey model, Ecol. Complex. 20 (2014), 248–256. https://doi.org/10.1016/j.ecocom.2014.04.001.

[6] D. Mukherjee, The effect of prey refuges on a three species food chain model, Differ. Equ. Dyn. Syst. 22 (2013), 413–426. https://doi.org/10.1007/s12591-013-0196-0.

[7] D. Mukherjee, The effect of refuge and immigration in a predator–prey system in the presence of a competitor for the prey, Nonlinear Anal.: Real World Appl. 31 (2016), 277–287. https://doi.org/10.1016/j.nonrwa.2016.02.004.

[8] R.K. Naji, S.J. Majeed, The dynamical analysis of a prey-predator model with a refuge-stage structure prey population, Int. J. Differ. Equ. 2016 (2016), 2010464. https://doi.org/10.1155/2016/2010464.

[9] D. Mukherjee, Study of refuge use on a predator–prey system with a competitor for the prey, Int. J. Biomath. 10 (2017), 1750023. https://doi.org/10.1142/s1793524517500231.

[10] A.S. Abdulghafour, R.K. Naji, A study of a diseased prey-predator model with refuge in prey and harvesting from predator, J. Appl. Math. 2018 (2018), 2952791. https://doi.org/10.1155/2018/2952791.

[11] D. Mukherjee, C. Maji, Bifurcation analysis of a Holling type II predator-prey model with refuge, Chinese J. Phys. 65 (2020), 153–162. https://doi.org/10.1016/j.cjph.2020.02.012.

[12] H.A. Ibrahim, D.K. Bahlool, H.A. Satar, et al. Stability and bifurcation of a prey-predator system incorporating fear and refuge. Commun. Math. Biol. Neurosci. 2022, (2022), 32. https://doi.org/10.28919/cmbn/7260.

[13] A.R.M. Jamil, R.K. Naji, Modeling and analysis of the influence of fear on the harvested modified Leslie–Gower

model involving nonlinear prey refuge, Mathematics. 10 (2022), 2857. https://doi.org/10.3390/math10162857.

[14] G.A. Polis, The evolution and dynamics of intraspecific predation, Ann. Rev. Ecol. Syst. 12 (1981), 225–251. https://www.jstor.org/stable/2097111.

[15] C. Kohlmeier, W. Ebenhöh, The stabilizing role of cannibalism in a predator-prey system, Bull. Math. Biol. 57 (1995), 401–411. https://doi.org/10.1007/bf02460632.

[16] P. Getto, O. Diekmann, A.M. de Roos, On the (dis) advantages of cannibalism, J. Math. Biol. 51 (2005), 695–712. https://doi.org/10.1007/s00285-005-0342-6.

[17] B. Buonomo, D. Lacitignola, On the stabilizing effect of cannibalism in stage-structured population models, Math. Biosci. Eng. 3 (2006), 717–731. https://doi.org/10.3934/mbe.2006.3.717.

[18] R. Marik, L. Pribylova, An age-structured model of cannibalism, Electron. J. Differ. Equ. 2006 (2006), 106.

[19] S. Biswas, S. Chatterjee, J. Chattopadhyay, Cannibalism may control disease in predator population: result drawn from a model based study, Math. Meth. Appl. Sci. 38 (2014), 2272–2290. https://doi.org/10.1002/mma.3220.

[20] A. Basheer, E. Quansah, S. Bhowmick, et al. Prey cannibalism alters the dynamics of Holling–Tanner-type predator–prey models, Nonlinear Dyn. 85 (2016), 2549–2567. https://doi.org/10.1007/s11071-016-2844-8.

[21] Y. Jia, Y. Li, J. Wu, Effect of predator cannibalism and prey growth on the dynamic behavior for a predator-stage structured population model with diffusion, J. Math. Anal. Appl. 449 (2017), 1479–1501. https://doi.org/10.1016/j.jmaa.2016.12.036.

[22] H. Deng, F. Chen, Z. Zhu, Z. Li, Dynamic behaviors of Lotka–Volterra predator–prey model incorporating predator cannibalism, Adv. Differ. Equ. 2019 (2019), 359. https://doi.org/10.1186/s13662-019-2289-8.

[23] S. Creel, D. Christianson, Relationships between direct predation and risk effects, Trends Ecol. Evol. 23 (2008), 194–201. https://doi.org/10.1016/j.tree.2007.12.004.

[24] N.H. Fakhry, R.K. Naji, The dynamics of a square root prey-predator model with fear, Iraqi J. Sci. 61 (2020), 139–146. https://doi.org/10.24996/ijs.2020.61.1.15.

[25] K. Sarkar, S. Khajanchi, Impact of fear effect on the growth of prey in a predator-prey interaction model, Ecol. Complex. 42 (2020), 100826. https://doi.org/10.1016/j.ecocom.2020.100826.

[26] S.K. Sasmal, Y. Takeuchi, Dynamics of a predator-prey system with fear and group defense, J. Math. Anal. Appl. 481 (2020), 123471. https://doi.org/10.1016/j.jmaa.2019.123471.

[27] F.H. Maghool, R.K. Naji, The dynamics of a tritrophic Leslie-Gower food-web system with the effect of fear, J. Appl. Math. 2021 (2021), 2112814. https://doi.org/10.1155/2021/2112814.

[28] J. Liu, P. Lv, B. Liu, et al. Dynamics of a predator-prey model with fear effect and time delay, Complexity. 2021 (2021), 9184193. https://doi.org/10.1155/2021/9184193.

[29] S. Vinoth, R. Sivasamy, K. Sathiyanathan, et al. The dynamics of a Leslie type predator–prey model with fear and Allee effect, Adv. Differ. Equ. 2021 (2021), 338. https://doi.org/10.1186/s13662-021-03490-x.

[30] S.A. Rahi, S. Kurnaz, R.K. Naji, The impact of fear on a stage structure prey–predator system with anti-predator behavior, Appl Nanosci. (2022). https://doi.org/10.1007/s13204-021-02160-4.

[31] É. Diz-Pita, M.V. Otero-Espinar, Predator–prey models: A review of some recent advances, Mathematics. 9 (2021), 1783. https://doi.org/10.3390/math9151783.

[32] M. Rayungsari, A. Suryanto, W.M. Kusumawinahyu, et al. Dynamical analysis of a predator-prey model incorporating predator cannibalism and refuge, Axioms 11 (2022), 116. https://doi.org/10.3390/axioms11030116.

[33] L. Perko, Differential equations and dynamical systems, Springer, New York, 3rd edition, 2001.

[34] T.C. Gard, Uniform persistence in multispecies population models, Math. Biosci. 85 (1987), 93–104. https://doi.org/10.1016/0025-5564(87)90101-5.